
ZO-AdaMM: Zeroth-Order Adaptive Momentum Method for Black-Box Optimization

Xiangyi Chen^{1,*} Sijia Liu^{2,*} Kaidi Xu^{3,*} Xingguo Li^{4,*}
 Xue Lin³ Mingyi Hong¹ David Cox²

¹University of Minnesota, USA

²MIT-IBM Watson AI Lab, IBM Research, USA

³Northeastern University, USA

⁴Princeton University, USA

Abstract

The adaptive momentum method (AdaMM), which uses past gradients to update descent directions and learning rates simultaneously, has become one of the most popular first-order optimization methods for solving machine learning problems. However, AdaMM is not suited for solving black-box optimization problems, where explicit gradient forms are difficult or infeasible to obtain. In this paper, we propose a zeroth-order AdaMM (ZO-AdaMM) algorithm, that generalizes AdaMM to the gradient-free regime. We show that the convergence rate of ZO-AdaMM for both convex and nonconvex optimization is roughly a factor of $O(\sqrt{d})$ worse than that of the first-order AdaMM algorithm, where d is problem size. In particular, we provide a deep understanding on why Mahalanobis distance matters in convergence of ZO-AdaMM and other AdaMM-type methods. As a byproduct, our analysis makes the first step toward understanding adaptive learning rate methods for nonconvex constrained optimization. Furthermore, we demonstrate two applications, designing per-image and universal adversarial attacks from black-box neural networks, respectively. We perform extensive experiments on ImageNet and empirically show that ZO-AdaMM converges much faster to a solution of high accuracy compared with 6 state-of-the-art ZO optimization methods.

1 Introduction

The development of gradient-free optimization methods has become increasingly important to solve many machine learning problems in which explicit expressions of the gradients are expensive or infeasible to obtain [1–7]. *Zeroth-Order (ZO)* optimization methods, one type of gradient-free optimization methods, mimic first-order (FO) methods but approximate the full gradient (or stochastic gradient) through random gradient estimates, given by the difference of function values at random query points [8, 9]. Compared to Bayesian optimization, derivative-free trust region methods, genetic algorithms and other types of gradient-free methods [10–13], ZO optimization has two main advantages: a) ease of implementation, via slight modification of commonly-used gradient-based algorithms, and b) comparable convergence rates to first-order algorithms.

Due to the stochastic nature of ZO optimization, which arises from both data sampling and random gradient estimation, existing ZO methods suffer from large variance of the noisy gradient compared to FO stochastic methods [14]. In practice, this causes poor convergence performance and/or function query efficiency. To partially mitigate these issues, ZO sign-based SGD (ZO-signSGD) was proposed by [14] with the rationale that taking the sign of random gradient estimates (i.e., normalizing gradient estimates elementwise) as the descent direction improves the robustness of gradient estimators

*Equal contribution.

to stochastic noise. Although ZO-signSGD has faster convergence speed than many existing ZO algorithms, it is only guaranteed to converge to a neighborhood of a solution. In the FO setting, taking the sign of a stochastic gradient as the descent direction gives rise to signSGD [15]. The use of sign of stochastic gradients also appears in adaptive momentum methods (AdaMM) such as Adam [16], RMSProp [17], AMSGrad [18], Padam [19], and AdaFom [20]. Indeed, it has been suggested by [21] that AdaMM enjoy dual advantages of sign descent and variance adaption.

Considering the motivation of ZO-signSGD and the success of AdaMM in FO optimization, one question arises: Can we generalize AdaMM to the ZO regime? To answer this question, we develop the zeroth-order adaptive momentum method (ZO-AdaMM) and analyze its convergence properties in both convex and nonconvex settings for constrained optimization.

Contributions *Theoretically*, for both convex and nonconvex optimization, we show that ZO-AdaMM is roughly a factor of $O(\sqrt{d})$ worse than that of the FO AdaMM algorithm, where d is the number of optimization variables. We also show that the *Euclidean* projection based AdaMM-type methods could suffer non-convergence issues for constrained optimization. This highlights the necessity of *Mahalanobis distance* based projection. And we establish the Mahalanobis distance based convergence analysis, which makes the first step toward understanding adaptive learning rate methods for nonconvex constrained optimization.

Practically, we formalize the experimental comparison of ZO-AdaMM with 6 state-of-the-art ZO algorithms in the application of black-box adversarial attacks to generate both per-image and universal adversarial perturbations. Our proposal could provide an experimental benchmark for future studies on ZO optimization. Code to reproduce experiments is released at the anonymous link <https://github.com/KaidiXu/ZO-AdaMM>.

Related work Many types of ZO algorithms have been developed, and their convergence rates have been rigorously studied under different problem settings. We highlight some recent works as below. For unconstrained stochastic optimization, ZO stochastic gradient descent (ZO-SGD) [9] and ZO stochastic coordinate descent (ZO-SCD) [22] were proposed, which have $O(\sqrt{d}/\sqrt{T})$ convergence rate, where T is the number of iterations. Compared to FO stochastic algorithms, ZO optimization suffers a slowdown dependent on the variable dimension d , e.g., $O(\sqrt{d})$ for ZO-SGD and ZO-SCD. In [23], the tightness of the dimension-dependent factor $O(\sqrt{d})$ has been proved in the framework of ZO stochastic mirror descent (ZO-SMD). In order to further improve the iteration complexity of ZO algorithms, the technique of variance reduction was applied to ZO-SGD and ZO-SCD, leading to ZO stochastic variance reduced algorithms with an improved convergence rate in T , namely, $O(d/T)$ [24–26]. This improvement is aligned with ZO gradient descent (ZO-GD) for deterministic nonconvex programming [8]. Moreover, ZO versions of proximal SGD (ProxSGD) [27], Frank-Wolfe (FW) [28, 2, 29], and online alternating direction method of multipliers (OADMM) [1, 30] have been developed for constrained optimization. Aside from the recent works on ZO algorithms mentioned before, there is rich literature in derivative-free optimization (DFO). Traditional DFO methods can be classified into direct search-based methods and model-based methods. Both the two type of methods are mostly iterative methods. The difference is that direct search-based methods refines its search direction based on the queried function values directly, while a model-based method builds a model that approximates the function to be optimized and updates the search direction based on the model. Representative methods of developed in DFO literature include NOMAD [31, 32], PSWarm [33], Cobyła [34], and BOBYQA [35]. More comprehensive discussion on DFO methods can be found in [36, 37].

2 Preliminaries: Gradient Estimation via ZO Oracle

The ZO gradient estimate of a function f is constructed by the forward difference of two function values at a random unit direction:

$$\hat{\nabla} f(\mathbf{x}) = (d/\mu)[f(\mathbf{x} + \mu\mathbf{u}) - f(\mathbf{x})]\mathbf{u}, \quad (1)$$

where \mathbf{u} is a random vector drawn uniformly from the sphere of a unit ball, and $\mu > 0$ is a small step size, known as the smoothing parameter. In many existing work such as [8, 9], the random direction vector \mathbf{u} was drawn from the standard Gaussian distribution. Here the use of uniform distribution ensures that the ZO gradient estimate (1) is defined in a bounded space rather than the whole real space required for Gaussian. As will be evident later, the boundedness of random gradient estimates is one of important conditions in the convergence analysis of ZO-AdaMM.

The rationale behind the ZO gradient estimate (1) is that although it is a biased approximation to the true gradient of f , it is *unbiased* to the gradient of the randomized smoothing version of f with parameter μ [23, 24, 30], i.e.,

$$f_\mu(\mathbf{x}) = \mathbb{E}_{\mathbf{u} \sim U_B} [f(\mathbf{x} + \mu \mathbf{u})], \quad (2)$$

where $\mathbf{u} \sim U_B$ denotes the uniform distribution over the unit Euclidean ball B . We review properties of the smoothing function (2) and connections to the ZO gradient estimator (1) in Appendix 1.

3 AdaMM from First to Zeroth Order

Consider a stochastic optimization problem of the generic form

$$\min_{\mathbf{x} \in \mathcal{X}} f(\mathbf{x}) = \mathbb{E}_\xi [f(\mathbf{x}; \xi)], \quad (3)$$

where $\mathbf{x} \in \mathbb{R}^d$ are optimization variables, \mathcal{X} is a closed convex set, f is a differentiable (possibly nonconvex) objective function, and ξ is a certain random variable that captures environmental uncertainties. In problem (3), if ξ obeys a uniform distribution built on empirical samples $\{\xi_i\}_{i=1}^n$, then we recover a finite-sum formulation with the objective function $f(\mathbf{x}) = \frac{1}{n} \sum_{i=1}^n f(\mathbf{x}; \xi_i)$.

First-order AdaMM in terms of AMSGrad [18]. We specify the algorithmic framework of AdaMM by AMSGrad [18], a modified version of Adam [16] with convergence guarantees for both convex and nonconvex optimization. In the algorithm, the descent direction \mathbf{m}_t is given by an exponential moving average of the past gradients. The learning rate r_t is adaptively penalized by a square root of exponential moving averages of squared past gradients. It has been proved in [18, 20, 38, 39] that AdaMM can reach $O(1/\sqrt{T})^2$ convergence rate. Here we omit its possible dependency on d for simplicity, but more accurate analysis will be provided later in Section 4 and 5.

ZO-AdaMM. By integrating AdaMM with the random gradient estimator (1), we obtain ZO-AdaMM in Algorithm 1. Here the square root, the square, the maximum, and the division operators are taken elementwise. Also, $\Pi_{\mathcal{X}, \mathbf{H}}(\mathbf{a})$ denotes the projection operation under Mahalanobis distance with respect to \mathbf{H} , i.e., $\arg \min_{\mathbf{x} \in \mathcal{X}} \|\sqrt{\mathbf{H}}(\mathbf{x} - \mathbf{a})\|_2^2$. If $\mathcal{X} = \mathbb{R}^d$, the projection step simplifies to $\mathbf{x}_{t+1} = \mathbf{x}_t - \alpha_t \hat{\mathbf{V}}_t^{-1/2} \mathbf{m}_t$. Clearly, $\alpha_t \hat{\mathbf{V}}_t^{-1/2}$ and \mathbf{m}_t can be interpreted as the adaptive learning rate and the momentum-type descent direction, which adopt exponential moving averages as follows,

Algorithm 1 ZO-AdaMM

Input: $\mathbf{x}_1 \in \mathcal{X}$, step sizes $\{\alpha_t\}_{t=1}^T$, $\beta_{1,t}$, $\beta_2 \in (0, 1]$, and set \mathbf{m}_0 , \mathbf{v}_0 and $\hat{\mathbf{v}}_0$
for $t = 1, 2, \dots, T$ **do**
 let $\hat{\mathbf{g}}_t = \hat{\nabla} f_t(\mathbf{x}_t)$ by (1), $f_t(\mathbf{x}_t) := f(\mathbf{x}_t; \xi_t)$
 $\mathbf{m}_t = \beta_{1,t} \mathbf{m}_{t-1} + (1 - \beta_{1,t}) \hat{\mathbf{g}}_t$
 $\mathbf{v}_t = \beta_2 \mathbf{v}_{t-1} + (1 - \beta_2) \hat{\mathbf{g}}_t^2$
 $\hat{\mathbf{v}}_t = \max(\hat{\mathbf{v}}_{t-1}, \mathbf{v}_t)$, and $\hat{\mathbf{V}}_t = \text{diag}(\hat{\mathbf{v}}_t)$
 $\mathbf{x}_{t+1} = \Pi_{\mathcal{X}, \sqrt{\hat{\mathbf{V}}_t}}(\mathbf{x}_t - \alpha_t \hat{\mathbf{V}}_t^{-1/2} \mathbf{m}_t)$
end for

$$\mathbf{m}_t = \sum_{j=1}^t \left[\left(\prod_{k=1}^{t-j} \beta_{1,t-k+1} \right) (1 - \beta_{1,j}) \hat{\mathbf{g}}_j \right], \quad \mathbf{v}_t = (1 - \beta_2) \sum_{j=1}^t (\beta_2^{t-j} \hat{\mathbf{g}}_j^2). \quad (4)$$

Here we assume that $\mathbf{m}_0 = \mathbf{0}$, $\mathbf{v}_0 = \mathbf{0}$ and $0^0 = 1$ by convention, and let $\hat{\mathbf{g}}_t = \hat{\nabla} f_t(\mathbf{x}_t)$ by (1) with $f_t(\mathbf{x}_t) := f(\mathbf{x}_t; \xi_t)$.

Motivation and rationale behind ZO-AdaMM. First, gradient normalization helps noise reduction in ZO optimization as shown by [6, 14]. In the similar spirit, ZO-AdaMM also normalizes the descent direction \mathbf{m}_t by $\sqrt{\hat{\mathbf{v}}_t}$. Particularly, compared to AdaMM, ZO-AdaMM prefers a small value of β_2 in practice, implying a strong favor to normalize the current gradient estimate; see Fig A1 in Appendix. In the extreme case of $\beta_{1,t} = \beta_2 \rightarrow 0$ and $\hat{\mathbf{v}}_t = \mathbf{v}_t$, ZO-AdaMM could reduce to ZO-signSGD [14] since $\hat{\mathbf{V}}_t^{-1/2} \mathbf{m}_t = \mathbf{m}_t / \sqrt{\mathbf{v}_t} = \hat{\mathbf{g}}_t / \sqrt{\hat{\mathbf{g}}_t^2} = \text{sign}(\hat{\mathbf{g}}_t)$ known from (4). However, the downside of ZO-signSGD is its worse convergence accuracy than ZO-SGD, i.e., it only converges to a neighborhood of a stationary point even for unconstrained optimization. Compared to ZO-signSGD, ZO-AdaMM is able to cover ZO-SGD as a special case when $\beta_{1,t} = 0$, $\beta_2 = 1$, $\mathbf{v}_0 = \mathbf{1}$ and $\hat{\mathbf{v}}_0 \leq \mathbf{1}$ from Algorithm 1. Thus, we hope that with appropriate choices of $\beta_{1,t}$ and β_2 , ZO-AdaMM could enjoy dual advantages of ZO-signSGD and ZO-SGD. Another motivation comes from the possible presence of time-dependent gradient priors [40]. Given this, the use of past gradients in momentum also helps noise reduction.

²In the paper, we could omit $\log(T)$ in Big O notation.

Why is ZO-AdaMM difficult to analyze? The convergence analysis of ZO-AdaMM becomes significantly more challenging than existing ZO methods due to the involved coupling among stochastic sampling, ZO gradinet estimation, momentum, adaptive learning rate, and projection operation. In particular, the use of Mahalanobis distance in projection step plays a key role on convergence guarantees. And the conventional variance bound on ZO gradient estimates is insufficient to analyze the convergence of ZO-AdaMM due to the use of adaptive learning rate. In the next sections, we will carefully study the convergence of ZO-AdaMM under different settings.

4 Convergence Analysis of ZO-AdaMM for Nonconvex Optimization

In this section, we begin by providing a deep understanding on the importance of Mahalanobis distance used in ZO-AdaMM (Algorithm 1), and then introduce the Mahalanobis distance based convergence analysis for both unconstrained and constrained nonconvex optimization. Our analysis makes the first step toward understanding adaptive learning rate methods for nonconvex constrained optimization. Throughout the section, we make the following assumptions.

A1: $f_t(\cdot) := f(\cdot; \xi_t)$ has L_g -Lipschitz continuous gradient, where $L_g > 0$.

A2: f_t has η -bounded stochastic gradient $\|\nabla f_t(\mathbf{x})\|_\infty \leq \eta$.

4.1 Importance of Mahalanobis distance based projection operation

Recall from Algorithm 1 that ZO-AdaMM takes the projection operation $\Pi_{\mathcal{X}, \sqrt{\hat{\mathbf{V}}_t}}(\cdot)$ onto the constraint set \mathcal{X} under Mahalanobis distance with respect to (w.r.t.) $\hat{\mathbf{V}}_t$. In some recent adversarial learning algorithms [41, 42], the Euclidean projection $\Pi_{\mathcal{X}}(\cdot)$ was used in both FO and ZO AdaMM-type methods rather than the Mahalanobis distance based projection in Algorithm 1. However, such an implementation could lead to *non-convergence*: Proposition 1 shows the non-convergence issue of Algorithm 1 using the Euclidean projection operation when solving a simple linear program subject to ℓ_1 -norm constraint. This is an important point which is ignored in design of many algorithms on adversarial training [43].

Proposition 1 *Consider the following problem*

$$\underset{\mathbf{x}=[x_1, x_2]^T}{\text{minimize}} \quad -2x_1 - x_2; \quad \text{subject to } |x_1 + x_2| \leq 1, \quad (5)$$

then Algorithm 1, initialized by $\mathbf{x} = [0.5, 0.5]^T$, using the Euclidean projection $\Pi_{\mathcal{X}}(\cdot)$ converges to a fixed point $[0.5, 0.5]^T$ rather than a stationary point of (5).

Proof: *The proof investigates a special case of Algorithm 1, projected signSGD; See Appendix 2.1.*

Proposition 1 indicates that replacing the Mahalanobis distance based projection in Algorithm 1 with Euclidean projection will lead to a divergent algorithm, highlighting the importance of using Mahalanobis distance. However, the use of Mahalanobis distance based projection complicates the convergence analysis, especially in constrained optimization. Accordingly, we define a Mahalanobis based convergence measure that can simplify the analysis and can be converted into the traditional convergence measure.

Let $\mathbf{x}^+ = \mathbf{x}_{t+1}$, $\mathbf{x}^- = \mathbf{x}_t$, $\mathbf{g} = \mathbf{m}_t$, $\omega = \alpha_t$ and $\mathbf{H} = \hat{\mathbf{V}}_t^{1/2}$, the projection step of Algorithm 1 can be written in the generic form

$$\mathbf{x}^+ = \arg \min_{\mathbf{x} \in \mathcal{X}} \{\langle \mathbf{g}, \mathbf{x} \rangle + (1/\omega) D_{\mathbf{H}}(\mathbf{x}, \mathbf{x}^-)\}, \quad (6)$$

where $D_{\mathbf{H}}(\mathbf{x}, \mathbf{x}^-) = \|\mathbf{H}^{1/2}(\mathbf{x} - \mathbf{x}^-)\|^2/2$ gives the Mahalanobis distance w.r.t. \mathbf{H} , and $\|\cdot\|$ denotes ℓ_2 norm. Based on (6), the concept of *gradient mapping* [27] is given by

$$P_{\mathcal{X}, \mathbf{H}}(\mathbf{x}^-, \mathbf{g}, \omega) := (\mathbf{x}^- - \mathbf{x}^+)/\omega. \quad (7)$$

The gradient mapping $P_{\mathcal{X}, \mathbf{H}}(\mathbf{x}^-, \mathbf{g}, \omega)$ yields a natural interpretation: a projected version of \mathbf{g} at the point \mathbf{x}^- given the learning rate ω , yielding $\mathbf{x}^+ = \mathbf{x}^- - \omega P_{\mathcal{X}, \mathbf{H}}(\mathbf{x}^-, \mathbf{g}, \omega)$. We note that different from [27, 44], the gradient mapping in (7) is defined on the projection under the Mahalanobis distance $D_{\mathbf{H}}(\cdot, \cdot)$ rather than the Euclidean distance.

With the aid of (7), we propose the Mahalanobis distance based convergence measure for ZO-AdaMM:

$$\|\mathcal{G}(\mathbf{x}_t)\|^2 := \|\hat{\mathbf{V}}_t^{1/4} P_{\mathcal{X}, \hat{\mathbf{V}}_t^{1/2}}(\mathbf{x}_t, \nabla f(\mathbf{x}_t), \alpha_t)\|^2. \quad (8)$$

If $\mathcal{X} = \mathbb{R}^d$, then the convergence measure (8) reduces to

$$\|\hat{\mathbf{V}}_t^{-1/4} \nabla f(\mathbf{x}_t)\|^2, \quad (9)$$

which corresponds to the squared Euclidean norm of gradient in a linearly transformed coordinate system $\mathbf{y}_t = \hat{\mathbf{V}}_t^{1/4} \mathbf{x}_t$. As will be evident later, the measure (9) can be transformed to the conventional measure $\|\nabla f(\mathbf{x}_t)\|^2$ for unconstrained optimization.

We remark that Mahalanobis (M-) distance facilitates our convergence analysis in an equivalently transformed space, over which the analysis can be generalized from the conventional projected gradient descent framework. To get intuition, let us consider a simpler first-order case with the \mathbf{x} -descent step given by Algorithm 1 as $\beta_{1,t} = 0$ and $\mathcal{X} = \mathbb{R}^d$: $\mathbf{x}_{t+1} = \mathbf{x}_t - \alpha \hat{\mathbf{V}}_t^{-1/2} \nabla f(\mathbf{x}_t)$. Note that the ZO case is more involved but follows the same intuition. Upon defining $\mathbf{y}_t \triangleq \hat{\mathbf{V}}_t^{1/4} \mathbf{x}_t$, the \mathbf{x} -update can then be rewritten as the update rule in \mathbf{y} : $\mathbf{y}_{t+1} = \mathbf{y}_t - \alpha \hat{\mathbf{V}}_t^{-1/4} \nabla f(\mathbf{x}_t)$. Since $\nabla_{\mathbf{y}_t} f(\mathbf{x}_t) = \left(\frac{\partial \mathbf{x}_t}{\partial \mathbf{y}_t}\right)^T \nabla f(\mathbf{x}_t) = \hat{\mathbf{V}}_t^{-1/4} \nabla f(\mathbf{x}_t)$, the \mathbf{y} -update, $\mathbf{y}_{t+1} = \mathbf{y}_t - \alpha \nabla_{\mathbf{y}} f(\mathbf{x}_t)$, obeys the gradient descent framework. In the constrained case, a similar but more involved analysis can be made, showing that the *M-projection in the \mathbf{x} -coordinate system* is *equivalent to the Euclidean projection in the \mathbf{y} -coordinate system* which makes projected gradient descent applicable to the update in \mathbf{y} . By contrast, the direct use of *Euclidean projection in the \mathbf{x} -coordinate system* leads to *divergence* in ZO-AdaMM (Proposition 1).

4.2 Unconstrained nonconvex optimization

We next demonstrate the convergence analysis of ZO-AdaMM for unconstrained nonconvex optimization. In Proposition 2, we begin by exploring the relationship between the convergence measure (9) and ZO gradient estimates; *See Appendix 2.2 for proof.*

Proposition 2 *Suppose that A1-A2 hold and let $\mathcal{X} = \mathbb{R}^d$, $\hat{\mathbf{v}}_0^{1/2} \geq c\mathbf{1}$, $f_\mu(\mathbf{x}_1) - \min_{\mathbf{x}} f_\mu(\mathbf{x}) \leq D_f$, $\beta_{1,t} = \beta_1$, $\gamma := \beta_1/\beta_2 < 1$, $\mu = 1/\sqrt{Td}$, and $\alpha_t = 1/\sqrt{Td}$ in Algorithm 1, then ZO-AdaMM yields*

$$\begin{aligned} \mathbb{E} \left[\left\| \hat{\mathbf{V}}_R^{-1/4} \nabla f(\mathbf{x}_R) \right\|^2 \right] &\leq \frac{L_g^2 d}{2c T} + 2D_f \frac{\sqrt{d}}{\sqrt{T}} + \frac{L_g(4 + 5\beta_1^2)(1 - \beta_1)}{2(1 - \beta_1)^2(1 - \beta_2)(1 - \gamma)} \frac{\sqrt{d}}{\sqrt{T}} \\ &\quad + \frac{2}{c} \mathbb{E} \left[2\eta^2 + \frac{\eta \max_{t \in [T]} \{\|\hat{\mathbf{g}}_t\|_\infty\}}{1 - \beta_1} \right] \frac{d}{T}, \end{aligned} \quad (10)$$

where \mathbf{x}_R is picked uniformly randomly from $\{\mathbf{x}_t\}_{t=1}^T$, and $\hat{\mathbf{g}}_t = \hat{\nabla} f_t(\mathbf{x}_t)$ by (1).

Proposition 2 implies that the convergence rate of ZO-AdaMM has a dependency on ZO gradient estimates in terms of $G_{z_0} := \max_{t \in [T]} \{\|\hat{\mathbf{g}}_t\|_\infty\}$. Moreover, if we consider the FO AdaMM [20, 38] in which the ZO gradient estimate $\hat{\mathbf{g}}_t$ is replaced with the stochastic gradient, then one can simply assume $\max_{t \in [T]} \{\|\mathbf{g}_t\|_\infty\}$ to be a dimension-independent constant under A2. However, in the ZO setting, G_{z_0} is no longer independent of d . For example, it could be directly bounded by $\|\hat{\nabla} f(\mathbf{x})\|_2 \leq (d/\mu) \|f(\mathbf{x} + \mu \mathbf{u}) - f(\mathbf{x})\|_2 \leq dL_c$ under the following assumption:

A3: f_t is L_c -Lipschitz continuous.

In Proposition 3, we show that the dimension-dependency of G_{z_0} can be further improved by using sphere concentration results; *See Appendix 2.3 for proof.*

Proposition 3 *Under A3, $\max\{d, T\} \geq 3$, and given $\delta \in (0, 1)$, then with probability at least $1 - \delta$,*

$$\max_{t \in [T]} \{\|\hat{\mathbf{g}}_t\|_\infty\} \leq 2L_c \sqrt{d \log(dT/\delta)}. \quad (11)$$

Here we provide some insights on Proposition 3. Since the unit random vector used to define $\hat{\mathbf{g}}_t$ is uniformly sampled on a sphere, $\|\hat{\mathbf{g}}_t\|_\infty$ can be improved to $O(\sqrt{d})$ with high probability. This is a tight bound since when the function difference is a constant, the lower bound satisfies $\|\hat{\mathbf{g}}_t\|_\infty = \Omega(\sqrt{d})$ by sphere concentration. It is also not surprising that our bound (11) grows with T

since we bound the maximum $\|\hat{\mathbf{g}}_t\|_\infty$ over T realizations with high probability. The time-dependence is required to compensate the growth of the probability that there exists an estimate with the extreme ℓ_∞ value versus time. Note that as long as T has polynomial rather than exponential dependency on d , we then always have $\max_{t \in [T]} \{\|\hat{\mathbf{g}}_t\|_\infty\} = O(\sqrt{d \log(d)})$. Based on Proposition 2 and Proposition 3, the convergence rate of ZO-AdaMM is provided by Theorem 1; *See Appendix 2.4 for proof.*

Theorem 1 *Suppose that **A1** and **A3** hold. Given parameter settings in Proposition 2 and 3, then with probability at least $1 - 1/(T\sqrt{d})$, ZO-AdaMM yields*

$$\mathbb{E} \left[\left\| \hat{\mathbf{V}}_R^{-1/4} \nabla f(\mathbf{x}_R) \right\|^2 \right] = O \left(\sqrt{d}/\sqrt{T} + d^{1.5}/T \right). \quad (12)$$

We can also extend the convergence rate of ZO-AdaMM in Theorem 1 using the measure $\mathbb{E}[\|\nabla f(\mathbf{x}_R)\|^2]$. Since $\hat{V}_{t,ii}^{-1/2} \geq 1/\max_{t \in [T]} \{\|\hat{\mathbf{g}}_t\|_\infty\}$ (by the update rule), we obtain from (11) that

$$\mathbb{E} [\|\nabla f(\mathbf{x}_R)\|^2] \leq 2L_c \sqrt{d \log(dT/\delta)} \mathbb{E} \left[\left\| \hat{\mathbf{V}}_R^{-1/4} \nabla f(\mathbf{x}_R) \right\|^2 \right]. \quad (13)$$

Theorem 1, together with (13), implies $O(d/\sqrt{T} + d^2/T)$ convergence rate of ZO-AdaMM under the conventional measure. We remark that compared to the FO rate $O(\sqrt{d}/\sqrt{T} + d/T)$ [38] of AdaMM for unconstrained nonconvex optimization under **A1-A2**, ZO-AdaMM suffers $O(\sqrt{d})$ and $O(d)$ slowdown on the rate term $O(1/\sqrt{T})$ and $O(1/T)$, respectively. This dimension-dependent slowdown is similar to ZO-SGD versus SGD shown by [9]. We also remark that compared to FO-AdaMM, ZO-AdaMM requires additional **A3** to bound the ℓ_∞ norm of ZO gradient estimates.

4.3 Constrained nonconvex optimization

To analyze ZO-AdaMM in a general constrained case, one needs to handle the coupling effects from all three factors: momentum, adaptive learning rate, and projection operation. Here we focus on addressing the coupling issue in the last two factors, which yields our results on ZO-AdaMM at $\beta_{1,t} = 0$. This is equivalent to the ZO version of RMSProp [17] with Reddi's convergence fix in [18]. When the momentum factor comes into play, the scenario becomes much more complicated. We leave the answer to the general case $\beta_{1,t} \neq 0$ for future research. Even for SGD with momentum, we are not aware of any successful convergence analysis for stochastic constrained nonconvex optimization.

It is known from SGD [27] that the presence of projection induces a stochastic bias (independent of iteration number T) for constrained nonconvex optimization. In Theorem 2, we show that the same challenge holds for ZO-AdaMM. Thus, one has to adopt the variance reduced gradient estimator, which induces higher querying complexity than the estimator (1); *See Appendix 2.5 for proof.*

Theorem 2 *Suppose that **A1-A2** hold, $\hat{\mathbf{v}}_0^{1/2} \geq c\mathbf{1}$, $f_\mu(\mathbf{x}_1) - \min_{\mathbf{x}} f_\mu(\mathbf{x}) \leq D_f$, $\alpha_t = \alpha \leq \frac{c}{L_g}$, $\mu = \frac{1}{\sqrt{Td}}$, and $\beta_{1,t} = 0$ in Algorithm 1, then the convergence rate of ZO-AdaMM under (8) satisfies*

$$\mathbb{E}[\|\mathcal{G}(\mathbf{x}_R)\|^2] \leq \frac{6D_f}{\alpha T} + \frac{3L_g^2 d}{4cT} + \frac{6\eta^2}{c^4 T} (\max_{t \in [T]} \mathbb{E}[\|\hat{\mathbf{g}}_t - f_\mu(\mathbf{x}_t)\|^2] + d\eta^2) + \frac{3c+9}{c} \max_{t \in [T]} \mathbb{E}[\|\hat{\mathbf{g}}_t - f_\mu(\mathbf{x}_t)\|^2],$$

where \mathbf{x}_R is picked uniformly randomly from $\{\mathbf{x}_t\}_{t=1}^T$, $\mathcal{G}(\mathbf{x})$ has been defined in (8), and f_μ is the smoothing function of f defined in (2).

Theorem 2 implies that regardless of the number of iterations T , ZO-AdaMM only converges to a solution's neighborhood whose size is determined by the variance of ZO gradient estimates $\max_{t \in [T]} \mathbb{E}[\|\hat{\mathbf{g}}_t - f_\mu(\mathbf{x}_t)\|^2]$. To make this term diminishing, we consider the following variance reduced gradient estimator built on multiple stochastic samples and random direction vectors [14],

$$\hat{\mathbf{g}}_t = \frac{1}{bq} \sum_{j \in \mathcal{I}_t} \sum_{i=1}^q \hat{\nabla} f(\mathbf{x}_t; \mathbf{u}_{i,t}, \boldsymbol{\xi}_j), \quad \hat{\nabla} f(\mathbf{x}_t; \mathbf{u}_{i,t}, \boldsymbol{\xi}_j) := \frac{d[f(\mathbf{x}_t + \mu \mathbf{u}_{i,t}; \boldsymbol{\xi}_j) - f(\mathbf{x}_t; \boldsymbol{\xi}_j)]}{\mu} \mathbf{u}_{i,t}, \quad (14)$$

where \mathcal{I}_t is a mini-batch containing b stochastic samples at time t , and $\{\mathbf{u}_{i,t}\}_{i=1}^q$ are q random direction vectors at time t . We present the variance of (14) in Lemma 1, whose proof is induced from [14, Proposition 2] by using $\|\nabla f_t\|_2^2 \leq d \|\nabla f_t\|_\infty^2 = d\eta^2$ in **A2**.

Lemma 1 Suppose that **A1-A2** hold, then for $\mu \leq 1/\sqrt{d}$, the variance of (14) yields

$$\mathbb{E} [\|\hat{\mathbf{g}}_t - \nabla f_\mu(\mathbf{x}_t)\|_2^2] = O(d/b + d^2/q). \quad (15)$$

Based on Lemma 1, the rate of ZO-AdaMM in Theorem 2 becomes $\mathbb{E}[\|\mathcal{G}(\mathbf{x}_R)\|^2] = O(d/T + d/b + d^2/q)$. Note that if **A3** holds, then the dimension-dependency can be improved by $O(d)$ factor based on Lemma 1. To the best of our knowledge, even in the FO case we are not aware of existing convergence rate analysis on adaptive learning rate methods for nonconvex constrained optimization.

5 Extended Analysis of ZO-AdaMM

ZO-AdaMM for constrained convex optimization Different from the nonconvex case, the convergence of ZO-AdaMM for convex optimization is commonly measured by the average regret $R_T = \mathbb{E} \left[\frac{1}{T} \sum_{t=1}^T f_t(\mathbf{x}_t) - \frac{1}{T} \sum_{t=1}^T f_t(\mathbf{x}^*) \right]$ [18, 19], where recall that $f_t(\mathbf{x}_t) = f(\mathbf{x}_t; \boldsymbol{\xi}_t)$, and \mathbf{x}^* is the optimal solution. We provide the average regret with the ZO gradient estimates by leveraging its connection to the smoothing function of f_t in Proposition 4; see Appendix 3.1 for proof.

Proposition 4 Suppose that $\alpha_t = \alpha/\sqrt{t}$, $\beta_{1,t} = \beta_1/t$ with $\beta_{1,1} = \beta_1$, $\beta_1, \beta_2 \in [0, 1)$, $\gamma := \beta_1/\sqrt{\beta_2} < 1$ and \mathcal{X} has bounded diameter D_∞ , then ZO-AdaMM for convex optimization yields

$$\begin{aligned} R_{T,\mu} &:= \mathbb{E} \left[\frac{1}{T} \sum_{t=1}^T f_{t,\mu}(\mathbf{x}_t) - \frac{1}{T} \sum_{t=1}^T f_{t,\mu}(\mathbf{x}^*) \right] \\ &\leq \frac{D_\infty^2 \sum_{i=1}^d \mathbb{E}[\hat{v}_{T,i}^{1/2}]}{\alpha(1-\beta_1)\sqrt{T}} + \frac{D_\infty^2}{2(1-\beta_1)T} \sum_{t=1}^T \sum_{i=1}^d \frac{\beta_1 \mathbb{E}[\hat{v}_{t,i}^{1/2}]}{\alpha\sqrt{t}} + \frac{\alpha\sqrt{1+\log T} \sum_{i=1}^d \mathbb{E}\|\hat{\mathbf{g}}_{1:T,i}\|}{(1-\beta_1)^2(1-\gamma)\sqrt{1-\beta_2}T}. \end{aligned} \quad (16)$$

where $f_{t,\mu}$ denotes the smoothing function of f defined by (2), $\hat{v}_{t,i}$ denotes the i th element of the vector $\hat{\mathbf{v}}_t$ defined in Algorithm 1, and $\hat{\mathbf{g}}_{1:T,i} := [\hat{g}_{1,i}, \dots, \hat{g}_{T,i}]^\top$.

We remark that Proposition 4 would reduce to [18, Theorem 4] by replacing ZO gradient estimates $\hat{\mathbf{g}}_{1:T,i}$ and $\hat{v}_{t,i}$ with FO gradients $\mathbf{g}_{1:T}$ and v_t . However, it was recently shown by [39] that the proof of [18, Theorem 4] is problematic. To address the proof issue, in Proposition 4 we present a simpler fix than [39, Theorem 4.1] and show that the conclusion of [18, Theorem 4] keeps correct. In the FO setting, the rate of AdaMM under **A2** for constrained convex optimization is given by $O(d/\sqrt{T})$ [19, Corollary 4.4]. Here **A2** provides the direct η -upper bound on $|g_{t,i}|$ and $\hat{v}_{t,i}^{1/2}$, and we consider worst-case rate analysis without imposing extra assumptions like sparse gradients³. In the ZO setting, we need further bound $|\hat{g}_{t,i}|$ and $\hat{v}_{t,i}$ and link $R_{T,\mu}$ to R_T , where the former is achieved by Proposition 3 and the latter is achieved by the relationship between f_t and its smoothing function $f_{t,\mu}$ shown in Lemma A1-(a), yielding $f_t(\mathbf{x}_t) - f_t(\mathbf{x}^*) \leq f_{t,\mu}(\mathbf{x}_t) - f_{t,\mu}(\mathbf{x}^*) + 2\mu L_c$. Thus, given $\mu \leq d/\sqrt{T}$ and assuming conditions in Proposition 3 hold, then the rate of ZO-AdaMM becomes $R_T \leq 2\mu L_c + R_{T,\mu} = O(d^{1.5}/\sqrt{T})$, which is $O(\sqrt{d})$ worse than the AdaMM.

Comparison with other ZO methods Since the existing convergence analysis for different ZO methods is built on different problem settings and assumptions. The direct comparison over the convergence rates might not be fair enough. Thus, in Table 1 we compare ZO-AdaMM with others ZO methods from 4 perspectives: a) the type of gradient estimator, b) the setting of smoothing parameter μ , c) convergence rate, and d) function query complexity.

Table 1 shows that for unconstrained nonconvex optimization, the convergence of ZO-AdaMM achieves worse dependency on d than ZO-SGD [9], ZO-SCD [22] and ZO-signSGD [14]. However, it has milder choice of μ than ZO-SGD, less query complexity than ZO-SCD, and no T -independent convergence bias compared to ZO-signSGD. Also, for constrained nonconvex optimization, ZO-AdaMM yields the similar rate to ZO-ProxSGD [27], which also implies ZO projected SGD (ZO-PSGD). For constrained convex optimization, the rate of ZO-AdaMM is $O(d)$ worse than ZO-SMD [23] but ours has the significantly improved dimension-dependency in μ . We also highlight that at the first glance, ZO-AdaMM has a worse d -dependency (regardless of choice of μ) than ZO-SGD. However, even in the FO setting, AdaMM has an extra $O(\sqrt{d})$ dependency in the worst case due to the effect of (coordinate-wise) gradient normalization when bounding the distance of two consecutive

³The work [40] showed the lack of sparsity in gradients while generating adversarial examples.

updates. Thus, in addition to comparing with different ZO methods, Table 1 also summarizes the convergence performance of FO AdaMM. Note that our rate yields $O(\sqrt{d})$ slowdown compared to FO AdaMM though bounding ZO gradient estimate norm requires stricter assumption.

| Method | Assumptions | Gradient estimator | Smoothing parameter μ | Rate | Query |
|---------------------------|---------------------------------------------------------------------------|-------------------------|---------------------------------------------------------|-----------------------------------------------------------------------------------------------|----------|
| ZO-SGD [9] | NC ¹ , UCons ¹ , A1 , A3 ² | GauGE ¹ | $O\left(\frac{1}{d\sqrt{T}}\right)$ | $O\left(\frac{\sqrt{d}}{\sqrt{T}} + \frac{d}{T}\right)$ | $O(T)$ |
| ZO-SCD [22] | NC, UCons, A1 , A3 ² | CooGE ¹ | $O\left(\frac{1}{\sqrt{T}} + \frac{1}{\sqrt{d}}\right)$ | $O\left(\frac{\sqrt{d}}{\sqrt{T}} + \frac{d}{T}\right)$ | $O(dT)$ |
| ZO-signSGD [14] | NC, UCons, A1 , A3 | sign-UniGE ¹ | $O\left(\frac{1}{\sqrt{dT}}\right)$ | $O\left(\frac{\sqrt{d}}{\sqrt{T}} + \frac{\sqrt{d}}{\sqrt{b}} + \frac{d}{\sqrt{bq}}\right)^3$ | $O(bqT)$ |
| ZO-ProxSGD / ZO-PSGD [27] | NC, Cons ⁴ , A1 , A3 | GauGE | $O\left(\frac{1}{\sqrt{dT}}\right)$ | $O\left(\frac{d^2}{qT} + \frac{d}{q}\right)$ | $O(qT)$ |
| ZO-SMD [23] | C, Cons, A3 | GauGE/UniGE | $O\left(\frac{1}{dt}\right)$ | $O\left(\frac{\sqrt{d}}{\sqrt{T}}\right)$ | $O(T)$ |
| AdaMM [20, 38] | NC, UCons, A1 , A2 | SGE ¹ | n/a | $O\left(\frac{\sqrt{d}}{\sqrt{T}} + \frac{d}{T}\right)$ | n/a |
| AdaMM [18, 19, 39] | C, Cons, A2 | SGE | n/a | $O\left(\frac{d}{\sqrt{T}}\right)$ | n/a |
| ZO-AdaMM | NC, UCons, A1 , A3 | UniGE | $O\left(\frac{1}{\sqrt{dT}}\right)$ | $O\left(\frac{d}{\sqrt{T}} + \frac{d^2}{T}\right)$ | $O(T)$ |
| ZO-AdaMM | NC, Cons, A1 , A3 $\beta_{1,t} = 0$ | UniGE | $O\left(\frac{1}{\sqrt{dT}}\right)$ | $O\left(\frac{d}{T} + \frac{1}{b} + \frac{d}{q}\right)$ | $O(bqT)$ |
| ZO-AdaMM | C, Cons, A3 | UniGE | $O\left(\frac{d}{\sqrt{T}}\right)$ | $O\left(\frac{d^{1.5}}{\sqrt{T}}\right)$ | $O(T)$ |

¹Abbreviations. NC: Nonconvex; UCons: Unconstrained; GauGE: Gaussian random vector based gradient estimate; UniGE: Uniform random vector based gradient estimate; CooGE: Coordinate-wise gradient estimate; SGE: stochastic (first-order) gradient estimate

²Assumption of bounded variance of stochastic gradients is implied from **A3**.

³Convergence of ZO-signSGD is measured by $\mathbb{E}[\|\nabla f(x_T)\|_2]$ rather than its square used in other algorithms for nonconvex optimization.

Table 1: Summary of convergence rate and query complexity of various ZO algorithms given T iterations.

6 Applications to Black-Box Adversarial Attacks

In this section, we demonstrate the effectiveness of ZO-AdaMM by experiments on generating black-box adversarial examples. Our experiments will be performed on Inception V3 [45] using ImageNet [46]. Here we focus on two types of black-box adversarial attacks: *per-image* adversarial perturbation [47] and *universal* adversarial perturbation against multiple images [5, 6, 48, 49]. For each type of attack, we allow both constrained and unconstrained optimization problem settings. We compare our proposed ZO-AdaMM method with 6 existing ZO algorithms: ZO-SGD, ZO-SCD and ZO-signSGD for unconstrained optimization, and ZO-PSGD, ZO-SMD and ZO-NES for constrained optimization. The first 5 methods have been summarized in Table 1, and ZO-NES refers to the black-box attack generation method in [6], which applies a projected version of ZO-signSGD using natural evolution strategy (NES) based random gradient estimator. In our experiments, every method takes the same number of queries per iteration. Accordingly, the total query complexity is consistent with the number of iterations. We refer to Appendix 4 for details on experiment setups.

Per-image adversarial perturbation In Fig. 1, we present the attack loss and the resulting ℓ_2 -distortion against iteration numbers for solving both unconstrained and constrained adversarial attack problems, namely, (94) and (93) in Appendix 4, over 100 randomly selected images. Here every algorithm is initialized by zero perturbation. Thus, as the iteration increases, the attack loss decreases until it converges to 0 (indicating successful attack) while the distortion could increase. At this sense, the best attack performance should correspond to the best tradeoff between the fast convergence to 0 attack loss and the low distortion power (evaluated by ℓ_2 norm). As we can see, ZO-AdaMM consistently outperforms other ZO methods in terms of the fast convergence of attack loss and relatively small perturbation. We also note that ZO-signSGD and ZO-NES have poor convergence accuracy in terms of either large attack loss or large distortion at final iterations. This is not surprising, since it has been shown in [14] that ZO-signSGD only converges to a neighborhood of a solution, and ZO-NES can be regarded as a Euclidean projection based ZO-signSGD, which could induce convergence issues shown by Prop. 1. We refer readers to Table A3 for detailed experiment results.

Universal adversarial perturbation We now focus on designing a universal adversarial perturbation using the constrained attack problem formulation. Here we attack $M = 100$ random selected images from ImageNet. In Fig. 2, we present the attack loss as well as the ℓ_2 norm of universal perturbation at different iteration numbers. As we can see, compared with the other ZO algorithms, ZO-AdaMM has the fastest convergence speed to reach the smallest adversarial perturbation (namely, strongest universal attack). Moreover, in Table 2 we present detailed attack success rate and ℓ_2 distortion over $T = 40000$ iterations. Consistent with Fig. 2, ZO-AdaMM achieves highest success rate

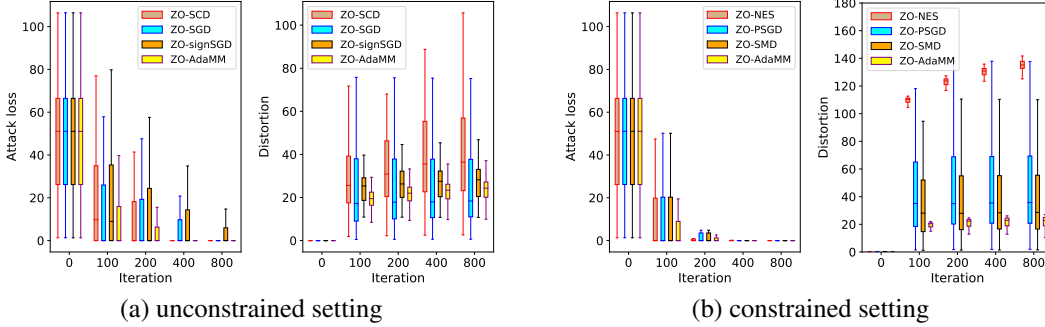


Figure 1: The attack loss and adversarial distortion v.s. iterations. Each box represents results from 100 images.

with lowest distortion. In Fig. A2 of Appendix A2, we visualize patterns of the generated universal adversarial perturbations which further confirm the advantage of ZO-AdaMM.

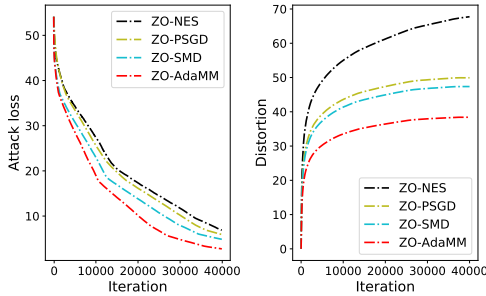


Figure 2: Attack loss and distortion of universal attack.

| Methods | Attack success rate | Final $\ \delta_T\ _2^2$ |
|----------|---------------------|--------------------------|
| ZO-NES | 74% | 67.74 |
| ZO-PSGD | 78% | 49.92 |
| ZO-SMD | 79% | 47.36 |
| ZO-AdaMM | 84% | 38.40 |

Table 2: Summary of attack success rate and eventual ℓ_2 distortion for universal attack against 100 images under $T = 40000$ iterations.

7 Conclusion

In this paper, we propose ZO-AdaMM, the first effort to integrate adaptive momentum methods with ZO optimization. In theory, we show that ZO-AdaMM has convergence guarantees for both convex and nonconvex constrained optimization. Compared with (first-order) AdaMM, it suffers a slowdown factor of $O(\sqrt{d})$. Particularly, we establish a new Mahalanobis distance based convergence measure whose necessity and importance are provided in characterizing the convergence behavior of ZO-AdaMM on nonconvex constrained problems. To demonstrate the utility of the algorithm, we show the superior performance of ZO-AdaMM for designing adversarial examples from black-box neural networks. Compared with 6 state-of-the-art ZO methods, ZO-AdaMM has the fastest empirical convergence to strong black-box adversarial attacks that require the minimum distortion strength.

References

- [1] S. Liu, J. Chen, P.-Y. Chen, and A. O. Hero, “Zeroth-order online ADMM: Convergence analysis and applications,” in *Proceedings of the Twenty-First International Conference on Artificial Intelligence and Statistics*, April 2018, vol. 84, pp. 288–297.
- [2] A. K. Sahu, M. Zaheer, and S. Kar, “Towards gradient free and projection free stochastic optimization,” *arXiv preprint arXiv:1810.03233*, 2018.
- [3] M. Feurer, A. Klein, K. Eggenberger, J. Springenberg, M. Blum, and F. Hutter, “Efficient and robust automated machine learning,” in *Advances in Neural Information Processing Systems*, 2015, pp. 2962–2970.
- [4] L. Kotthoff, C. Thornton, H. H. Hoos, F. Hutter, and K. Leyton-Brown, “Auto-weka 2.0: Automatic model selection and hyperparameter optimization in weka,” *J. Mach. Learn. Res.*, vol. 18, no. 1, pp. 826–830, Jan. 2017.

- [5] P.-Y. Chen, H. Zhang, Y. Sharma, J. Yi, and C.-J. Hsieh, “Zoo: Zeroth order optimization based black-box attacks to deep neural networks without training substitute models,” in *Proceedings of the 10th ACM Workshop on Artificial Intelligence and Security*. ACM, 2017, pp. 15–26.
- [6] A. Ilyas, K. Engstrom, A. Athalye, and J. Lin, “Black-box adversarial attacks with limited queries and information,” in *Proceedings of the 35th International Conference on Machine Learning*, July 2018.
- [7] C.-C. Tu, P. Ting, P.-Y. Chen, S. Liu, H. Zhang, J. Yi, C.-J. Hsieh, and S.-M. Cheng, “Autozoom: Autoencoder-based zeroth order optimization method for attacking black-box neural networks,” *arXiv preprint arXiv:1805.11770*, 2018.
- [8] Y. Nesterov and V. Spokoiny, “Random gradient-free minimization of convex functions,” *Foundations of Computational Mathematics*, vol. 2, no. 17, pp. 527–566, 2015.
- [9] S. Ghadimi and G. Lan, “Stochastic first-and zeroth-order methods for nonconvex stochastic programming,” *SIAM Journal on Optimization*, vol. 23, no. 4, pp. 2341–2368, 2013.
- [10] B. Shahriari, K. Swersky, Z. Wang, R. P. Adams, and N. De Freitas, “Taking the human out of the loop: A review of bayesian optimization,” *Proceedings of the IEEE*, vol. 104, no. 1, pp. 148–175, 2016.
- [11] A. R. Conn, K. Scheinberg, and L. Vicente, “Global convergence of general derivative-free trust-region algorithms to first-and second-order critical points,” *SIAM Journal on Optimization*, vol. 20, no. 1, pp. 387–415, 2009.
- [12] D. Whitley, “A genetic algorithm tutorial,” *Statistics and computing*, vol. 4, no. 2, pp. 65–85, 1994.
- [13] A. R. Conn, K. Scheinberg, and L. N. Vicente, *Introduction to derivative-free optimization*, vol. 8, Siam, 2009.
- [14] S. Liu, P.-Y. Chen, X. Chen, and M. Hong, “signSGD via zeroth-order oracle,” in *International Conference on Learning Representations*, 2019.
- [15] J. Bernstein, Y. Wang, K. Azizzadenesheli, and A. Anandkumar, “signsgd: compressed optimisation for non-convex problems,” *arXiv preprint arXiv:1802.04434*, 2018.
- [16] D. P. Kingma and J. Ba, “Adam: A method for stochastic optimization,” in *Proc. 3rd Int. Conf. Learn. Representations*, 2014.
- [17] T. Tieleman and G. Hinton, “Lecture 6.5-rmsprop: Divide the gradient by a running average of its recent magnitude,” *COURSERA: Neural networks for machine learning*, vol. 4, no. 2, pp. 26–31, 2012.
- [18] S. J. Reddi, S. Kale, and S. Kumar, “On the convergence of adam and beyond,” in *International Conference on Learning Representations*, 2018.
- [19] J. Chen and Q. Gu, “Closing the generalization gap of adaptive gradient methods in training deep neural networks,” *arXiv preprint arXiv:1806.06763*, 2018.
- [20] X. Chen, S. Liu, R. Sun, and M. Hong, “On the convergence of a class of adam-type algorithms for non-convex optimization,” *arXiv preprint arXiv:1808.02941*, 2018.
- [21] L. Balles and P. Hennig, “Dissecting adam: The sign, magnitude and variance of stochastic gradients,” in *Proceedings of the 35th International Conference on Machine Learning*, Jennifer Dy and Andreas Krause, Eds., Stockholmsmässan, Stockholm Sweden, 10–15 Jul 2018, vol. 80 of *Proceedings of Machine Learning Research*, pp. 404–413.
- [22] X. Lian, H. Zhang, C.-J. Hsieh, Y. Huang, and J. Liu, “A comprehensive linear speedup analysis for asynchronous stochastic parallel optimization from zeroth-order to first-order,” in *Advances in Neural Information Processing Systems*, 2016, pp. 3054–3062.
- [23] J. C. Duchi, M. I. Jordan, M. J. Wainwright, and A. Wibisono, “Optimal rates for zero-order convex optimization: The power of two function evaluations,” *IEEE Transactions on Information Theory*, vol. 61, no. 5, pp. 2788–2806, 2015.

- [24] S. Liu, B. Kailkhura, P.-Y. Chen, P. Ting, S. Chang, and L. Amini, “Zeroth-order stochastic variance reduction for nonconvex optimization,” *Advances in Neural Information Processing Systems*, 2018.
- [25] B. Gu, Z. Huo, and H. Huang, “Zeroth-order asynchronous doubly stochastic algorithm with variance reduction,” *arXiv preprint arXiv:1612.01425*, 2016.
- [26] L. Liu, M. Cheng, C.-J. Hsieh, and D. Tao, “Stochastic zeroth-order optimization via variance reduction method,” *arXiv preprint arXiv:1805.11811*, 2018.
- [27] S. Ghadimi, G. Lan, and H. Zhang, “Mini-batch stochastic approximation methods for non-convex stochastic composite optimization,” *Mathematical Programming*, vol. 155, no. 1-2, pp. 267–305, 2016.
- [28] Krishnakumar Balasubramanian and Saeed Ghadimi, “Zeroth-order (non)-convex stochastic optimization via conditional gradient and gradient updates,” in *Advances in Neural Information Processing Systems*, 2018, pp. 3455–3464.
- [29] J. Chen, J. Yi, and Q. Gu, “A Frank-Wolfe framework for efficient and effective adversarial attacks,” *arXiv preprint arXiv:1811.10828*, 2018.
- [30] X. Gao, B. Jiang, and S. Zhang, “On the information-adaptive variants of the ADMM: an iteration complexity perspective,” *Optimization Online*, vol. 12, 2014.
- [31] Sébastien Le Digabel, “Algorithm 909: Nomad: Nonlinear optimization with the mads algorithm,” *ACM Transactions on Mathematical Software (TOMS)*, vol. 37, no. 4, pp. 44, 2011.
- [32] Charles Audet and John E Dennis Jr, “Mesh adaptive direct search algorithms for constrained optimization,” *SIAM Journal on optimization*, vol. 17, no. 1, pp. 188–217, 2006.
- [33] A Ismael F Vaz and Luís N Vicente, “Pswarm: a hybrid solver for linearly constrained global derivative-free optimization,” *Optimization Methods & Software*, vol. 24, no. 4-5, pp. 669–685, 2009.
- [34] Michael JD Powell, “A direct search optimization method that models the objective and constraint functions by linear interpolation,” in *Advances in optimization and numerical analysis*, pp. 51–67. Springer, 1994.
- [35] Michael JD Powell, “The bobyqa algorithm for bound constrained optimization without derivatives,” *Cambridge NA Report NA2009/06, University of Cambridge, Cambridge*, pp. 26–46, 2009.
- [36] L. M. Rios and N. V. Sahinidis, “Derivative-free optimization: a review of algorithms and comparison of software implementations,” *Journal of Global Optimization*, vol. 56, no. 3, pp. 1247–1293, 2013.
- [37] Charles Audet and Warren Hare, *Derivative-free and blackbox optimization*, Springer, 2017.
- [38] D. Zhou, Y. Tang, Z. Yang, Y. Cao, and Q. Gu, “On the convergence of adaptive gradient methods for nonconvex optimization,” *arXiv preprint arXiv:1808.05671*, 2018.
- [39] T. T. Phuong and L. T. Phong, “On the convergence proof of amsgrad and a new version,” *arXiv preprint arXiv:1904.03590*, 2019.
- [40] A. Ilyas, L. Engstrom, and A. Madry, “Prior convictions: Black-box adversarial attacks with bandits and priors,” *arXiv preprint arXiv:1807.07978*, 2018.
- [41] A. Kurakin, I. Goodfellow, and S. Bengio, “Adversarial examples in the physical world,” *arXiv preprint arXiv:1607.02533*, 2016.
- [42] A. Ilyas, L. Engstrom, A. Athalye, and J. Lin, “Black-box adversarial attacks with limited queries and information,” *arXiv preprint arXiv:1804.08598*, 2018.
- [43] Aleksander Madry, Aleksandar Makelov, Ludwig Schmidt, Dimitris Tsipras, and Adrian Vladu, “Towards deep learning models resistant to adversarial attacks,” *arXiv preprint arXiv:1706.06083*, 2017.

- [44] S. J. Reddi, S. Sra, B. Póczos, and A. J. Smola, “Proximal stochastic methods for nonsmooth nonconvex finite-sum optimization,” in *Advances in Neural Information Processing Systems*, 2016, pp. 1145–1153.
- [45] C. Szegedy, V. Vanhoucke, S. Ioffe, J. Shlens, and Z. Wojna, “Rethinking the inception architecture for computer vision,” in *IEEE Conference on Computer Vision and Pattern Recognition (CVPR)*, 2016, pp. 2818–2826.
- [46] J. Deng, W. Dong, R. Socher, L.-J. Li, K. Li, and F.-F. Li, “Imagenet: A large-scale hierarchical image database,” in *Computer Vision and Pattern Recognition, 2009. CVPR 2009. IEEE Conference on*. IEEE, 2009, pp. 248–255.
- [47] Kaidi Xu, Sijia Liu, Pu Zhao, Pin-Yu Chen, Huan Zhang, Quanfu Fan, Deniz Erdogmus, Yanzhi Wang, and Xue Lin, “Structured adversarial attack: Towards general implementation and better interpretability,” in *International Conference on Learning Representations*, 2019.
- [48] F. Suya, Y. Tian, D. Evans, and P. Papotti, “Query-limited black-box attacks to classifiers,” *arXiv preprint arXiv:1712.08713*, 2017.
- [49] M. Cheng, T. Le, P.-Y. Chen, J. Yi, H. Zhang, and C.-J. Hsieh, “Query-efficient hard-label black-box attack: An optimization-based approach,” *arXiv preprint arXiv:1807.04457*, 2018.
- [50] S. Dasgupta and A. Gupta, “An elementary proof of a theorem of johnson and lindenstrauss,” *Random Struct. Algorithms*, vol. 22, no. 1, pp. 60–65, Jan. 2003.
- [51] N. Carlini and D. Wagner, “Towards evaluating the robustness of neural networks,” in *IEEE Symposium on Security and Privacy*, 2017, pp. 39–57.

Appendix

1 Smoothing Function and Random Gradient Estimate

Lemma A1 *a) Relationship between f_μ and f : If f is convex, then f_μ is convex. If f is L_c -Lipschitz continuous, then f_μ is L_c -Lipschitz continuous. Moreover for any $\mathbf{x} \in \mathbb{R}^d$,*

$$|f_\mu(\mathbf{x}) - f(\mathbf{x})| \leq L_c \mu. \quad (17)$$

If f has L_g -Lipschitz continuous gradient, then f_μ has L_g -Lipschitz continuous gradient. Moreover for any $\mathbf{x} \in \mathbb{R}^d$,

$$|f_\mu(\mathbf{x}) - f(\mathbf{x})| \leq L_g \mu^2 / 2 \quad (18)$$

$$\|\nabla f_\mu(\mathbf{x}) - \nabla f(\mathbf{x})\|_2^2 \leq \mu^2 d^2 L_g^2 / 4. \quad (19)$$

b) Statistical properties of $\hat{\nabla} f$: For any $\mathbf{x} \in \mathbb{R}^d$,

$$\mathbb{E}_{\mathbf{u}} \left[\hat{\nabla} f(\mathbf{x}) \right] = \nabla f_\mu(\mathbf{x}). \quad (20)$$

If f has L_g -Lipschitz continuous gradient, then

$$\mathbb{E}_{\mathbf{u}} \left[\|\hat{\nabla} f(\mathbf{x})\|_2^2 \right] \leq 2d \|\nabla f(\mathbf{x})\|_2^2 + \mu^2 L_g^2 d^2 / 2. \quad (21)$$

Proof: We refer readers to [30, Lemma 4.1] for the detailed proof of a)-b) except the Lipschitz continuity of f_μ and (17). Suppose that f is L_c -Lipschitz continuous, based on the definition of f_μ in (2), we obtain

$$|f_\mu(\mathbf{x}) - f_\mu(\mathbf{y})| \leq \frac{1}{\alpha(d)} \int_B |f(\mathbf{x} + \mu \mathbf{u}) - f(\mathbf{y} + \mu \mathbf{u})| d\mathbf{u} \leq L_c \|\mathbf{x} - \mathbf{y}\|_2,$$

where $\alpha(d)$ denotes the volume of the unit ball B in \mathbb{R}^d .

Moreover, we prove (17) as below.

$$|f_\mu(\mathbf{x}) - f(\mathbf{x})| = \left| \frac{1}{\alpha(d)} \int_B f(\mathbf{x} + \mu \mathbf{u}) - f(\mathbf{x}) d\mathbf{u} \right| \leq \frac{\mu L_c}{\alpha(d)} \int_B \|\mathbf{u}\|_2 d\mathbf{u} = \frac{\mu L_c d}{d+1} \leq \mu L_c,$$

where the first equality holds due to (2), Jensen's inequality and Lipschitz continuity of f , and the last equality holds since $(1/\alpha(d)) \int_B \|\mathbf{u}\|_2^2 d\mathbf{u} = \frac{n}{n+p}$ [30, Lemma 6.3.a]. \square

In Lemma A1, it is clear from (19) and (20) that the ZO gradient estimate (1) becomes unbiased to the true gradient ∇f only when $\mu \rightarrow 0$. However, if μ is too small, then the difference of empirical function values is also too small to represent the function differential [22, 24]. Thus, the tolerance on the smoothing parameter μ is an important factor to indicate the convergence performance of ZO optimization methods. It is also known from (21) that regardless of the value of μ , the variance of the ZO gradient estimate is always proportional to the dimension d . This is one of reasons for the dimension-dependent slowdown in convergence of ZO optimization methods. This also introduces technical difficulties for analyzing the effect of adaptive learning rate on the convergence of ZO-AdaMM in nonconvex optimization.

2 Proof for Nonconvex Optimization

2.1 Proof of Proposition 1

Let us consider a special case of Algorithm 1 with the average ZO gradient estimate $\hat{\nabla} f(\mathbf{x}) = \frac{d}{q\mu} \sum_{i=1}^q \{[f(\mathbf{x} + \mu \mathbf{u}_i) - f(\mathbf{x})] \mathbf{u}_i\}$ under $\beta_{1,t} = \beta_2 \rightarrow 0$, $\mu \rightarrow 0$ and $q \rightarrow \infty$. The conditions of $\beta_{1,t} = \beta_2 \rightarrow 0$ enables Algorithm 1 to reduce to ZO-signSGD in [14], and the conditions of $\mu \rightarrow 0$ and $q \rightarrow \infty$ makes the ZO gradient estimate unbiased to $\nabla f(\mathbf{x})$ and its variance close to 0 [14, Proposition 2]. As a result, we obtain $\hat{\mathbf{g}}_t \rightarrow \nabla f(\mathbf{x}_t)$, and Algorithm 1 becomes signSGD [15],

$$\mathbf{x}_{t+1} = \Pi_{\mathcal{X}, \mathbf{I}}(\mathbf{x}_t - \alpha_t \text{sign}(\nabla f(\mathbf{x}_t))) \quad (22)$$

where $\text{sign}(x) = 1$ if $x > 0$ and -1 if $x < 0$, and it is taken elementwise for a vector argument.

Let $f(\mathbf{x}) = -2x_1 - x_2$ in (5). We then run (22) at $x_1 = x_2 = 0.5$, which yields

$$\mathbf{x}_{t+1} = \Pi_{\mathcal{X}}([0.5, 0.5]^T - \alpha_t [-1, -1]^T) = \Pi_{\mathcal{X}}([0.5 + \alpha_t, 0.5 + \alpha_t]^T) = [0.5, 0.5]^T, \quad (23)$$

where \mathcal{X} encodes the constraint $|x_1 + x_2| \leq 1$.

It is clear that the updating rule (23) will converge to $\mathbf{x} = [0.5, 0.5]^T$ regardless of the choice of α_t . The remaining question is whether or not it is a stationary point. Recall that a point \mathbf{x}^* is a stationary point if it satisfies the following conditions:

$$\langle \nabla f(\mathbf{x}^*), \mathbf{x} - \mathbf{x}^* \rangle \geq 0, \forall \mathbf{x} \in \mathcal{X}. \quad (24)$$

Since the gradient at $[0.5, 0.5]^T$ is $[-2, -1]^T$, and the inequality (24) at $\mathbf{x} = [0.6, 0.4]^T \in X$ does *not* hold, given by $\langle [-2, -1]^T, [0.6, 0.4]^T - [0.5, 0.5]^T \rangle = -0.1 < 0$. This implies that $\mathbf{x}^* = [0.5, 0.5]^T$ is *not* a stationary point of problem (5).

Next, we apply the Mhalanobis distance $\hat{\mathbf{V}}_t = \text{diag}(\nabla f(\mathbf{x}_t)^2)$ to (22),

$$\mathbf{x}_{t+1} = \Pi_{\mathcal{X}, \hat{\mathbf{V}}_t^{1/2}}(\mathbf{x}_t - \alpha_t \text{sign}(\nabla f(\mathbf{x}_t))) = \Pi_{\mathcal{X}, \hat{\mathbf{V}}_t^{1/2}}(\mathbf{x}_t - \alpha_t \hat{\mathbf{V}}_t^{-1/2} \nabla f(\mathbf{x}_t)). \quad (25)$$

Similar to (22), we then consider the impact of fixed point $\mathbf{x}_{t+1} = \mathbf{x}_t$ on (25). By the definition of projection operator, we have

$$\mathbf{x}_t = \arg \min_{\mathbf{x} \in \mathcal{X}} \|\hat{\mathbf{V}}_t^{1/4}(\mathbf{x} - \mathbf{x}_t + \alpha_t \hat{\mathbf{V}}_t^{-1/2} \nabla f(\mathbf{x}_t))\| \quad (26)$$

The optimality condition of (26) is given by

$$\langle \hat{\mathbf{V}}_t^{1/2}(\mathbf{x}_t - \mathbf{x}_t + \alpha_t \hat{\mathbf{V}}_t^{-1/2} \nabla f(\mathbf{x}_t)), \mathbf{x} - \mathbf{x}_t \rangle \geq 0, \forall \mathbf{x} \in X,$$

which reduces to

$$\langle \nabla f(\mathbf{x}_t), \mathbf{x} - \mathbf{x}_t \rangle \geq 0, \forall \mathbf{x} \in X. \quad (27)$$

It thus means that \mathbf{x}_t is a stationary point by (24). \square

2.2 Proof of Proposition 2

Before proving the main result Proposition 2, we first prove a few auxiliary lemmas.

Lemma 2.1 *Given $\{\mathbf{x}_t\}$ from Algorithm 1, consider the sequence*

$$\mathbf{z}_t = \mathbf{x}_t + \frac{\beta_1}{1 - \beta_1}(\mathbf{x}_t - \mathbf{x}_{t-1}), \forall t \geq 1, \quad (28)$$

where let $\mathbf{x}_0 := \mathbf{x}_1$. Then for $\beta_{1,t} = \beta_1$ and $\mathcal{X} = \mathbb{R}^d$, $\forall t > 1$

$$\begin{aligned} & \mathbf{z}_{t+1} - \mathbf{z}_t \\ &= -\frac{\beta_1}{1 - \beta_1} \left(\alpha_t \hat{\mathbf{V}}_t^{-1/2} - \alpha_{t-1} \hat{\mathbf{V}}_{t-1}^{-1/2} \right) \mathbf{m}_{t-1} - \alpha_t \hat{\mathbf{V}}_t^{-1/2} \hat{\mathbf{g}}_t \end{aligned}$$

and

$$\mathbf{z}_2 - \mathbf{z}_1 = -\alpha_1 \hat{\mathbf{g}}_1 / \sqrt{\hat{\mathbf{v}}_1}.$$

Proof of Lemma 2.1: The proof follows from Lemma 6.1 in [20] by setting $\beta_{1,t} = \beta_1$.

Lemma 2.2 *By ZO-AdaMM update rule, we have*

$$\mathbb{E}[f_\mu(\mathbf{z}_{t+1}) - f_\mu(\mathbf{z}_1)] \leq \sum_{t=1}^T E[\langle \nabla f_\mu(\mathbf{x}_t), \mathbf{z}_{t+1} - \mathbf{z}_t \rangle] + \frac{4L_g + 5L_g\beta_1^2}{2(1 - \beta_1)^2} \sum_{t=1}^T E[\|\mathbf{x}_{t+1} - \mathbf{x}_t\|^2] \quad (29)$$

Proof of Lemma 2.2: By smoothness of function f , we can have

$$\begin{aligned}
& f_\mu(\mathbf{z}_{t+1}) - f_\mu(\mathbf{z}_t) \\
& \leq \langle \nabla f_\mu(\mathbf{z}_t), \mathbf{z}_{t+1} - \mathbf{z}_t \rangle + \frac{L_g}{2} \|\mathbf{z}_{t+1} - \mathbf{z}_t\|^2 \\
& = \langle \nabla f_\mu(\mathbf{x}_t), \mathbf{z}_{t+1} - \mathbf{z}_t \rangle + \frac{L_g}{2} \|\mathbf{z}_{t+1} - \mathbf{z}_t\|^2 + \langle \nabla f_\mu(\mathbf{z}_t) - \nabla f_\mu(\mathbf{x}_t), \mathbf{z}_{t+1} - \mathbf{z}_t \rangle \\
& \leq \langle \nabla f_\mu(\mathbf{x}_t), \mathbf{z}_{t+1} - \mathbf{z}_t \rangle + \frac{L_g}{2} \|\mathbf{z}_{t+1} - \mathbf{z}_t\|^2 + \frac{1}{2} \left(\frac{1}{L_g} \|\nabla f_\mu(\mathbf{z}_t) - \nabla f_\mu(\mathbf{x}_t)\|^2 + L_g \|\mathbf{z}_{t+1} - \mathbf{z}_t\|^2 \right) \\
& \leq \langle \nabla f_\mu(\mathbf{x}_t), \mathbf{z}_{t+1} - \mathbf{z}_t \rangle + L_g \|\mathbf{z}_{t+1} - \mathbf{z}_t\|^2 + \frac{1}{2} L_g \|\mathbf{z}_t - \mathbf{x}_t\|^2 \\
& = \langle \nabla f_\mu(\mathbf{x}_t), \mathbf{z}_{t+1} - \mathbf{z}_t \rangle + L_g \|\mathbf{z}_{t+1} - \mathbf{z}_t\|^2 + \frac{1}{2} L_g \frac{\beta_1}{1 - \beta_1} \|\mathbf{x}_t - \mathbf{x}_{t-1}\|^2 \tag{30}
\end{aligned}$$

Further, by (28), we have

$$\mathbf{z}_{t+1} - \mathbf{z}_t = \frac{1}{1 - \beta_1} (\mathbf{x}_{t+1} - \mathbf{x}_t) + \frac{\beta_1}{1 - \beta_1} (\mathbf{x}_t - \mathbf{x}_{t-1})$$

and thus

$$\|\mathbf{z}_{t+1} - \mathbf{z}_t\|^2 \leq \frac{2}{(1 - \beta_1)^2} \|\mathbf{x}_{t+1} - \mathbf{x}_t\|^2 + \frac{2\beta_1^2}{(1 - \beta_1)^2} \|\mathbf{x}_t - \mathbf{x}_{t-1}\|^2 \tag{31}$$

Substituting (31) into (30), we get

$$\begin{aligned}
& f_\mu(\mathbf{z}_{t+1}) - f_\mu(\mathbf{z}_t) \\
& \leq \langle \nabla f_\mu(\mathbf{x}_t), \mathbf{z}_{t+1} - \mathbf{z}_t \rangle + \frac{2L_g}{(1 - \beta_1)^2} \|\mathbf{x}_{t+1} - \mathbf{x}_t\|^2 + \frac{2\beta_1^2 L_g}{(1 - \beta_1)^2} \|\mathbf{x}_t - \mathbf{x}_{t-1}\|^2 \\
& \quad + \frac{1}{2} L_g \frac{\beta_1^2}{(1 - \beta_1)^2} \|\mathbf{x}_t - \mathbf{x}_{t-1}\|^2 \\
& = \langle \nabla f_\mu(\mathbf{x}_t), \mathbf{z}_{t+1} - \mathbf{z}_t \rangle + \frac{2L_g}{(1 - \beta_1)^2} \|\mathbf{x}_{t+1} - \mathbf{x}_t\|^2 + \frac{5L_g \beta_1^2}{2(1 - \beta_1)^2} \|\mathbf{x}_t - \mathbf{x}_{t-1}\|^2 \tag{32}
\end{aligned}$$

Summing t from 1 to T and take expectation, we get

$$\begin{aligned}
& \mathbb{E}[f_\mu(\mathbf{z}_{t+1}) - f_\mu(\mathbf{z}_1)] \\
& \leq \mathbb{E} \left[\sum_{t=1}^T \left(\langle \nabla f_\mu(\mathbf{x}_t), \mathbf{z}_{t+1} - \mathbf{z}_t \rangle + \frac{2L_g}{(1 - \beta_1)^2} \|\mathbf{x}_{t+1} - \mathbf{x}_t\|^2 + \frac{5L_g \beta_1^2}{2(1 - \beta_1)^2} \|\mathbf{x}_t - \mathbf{x}_{t-1}\|^2 \right) \right] \\
& \leq \sum_{t=1}^T \mathbb{E} [\langle \nabla f_\mu(\mathbf{x}_t), \mathbf{z}_{t+1} - \mathbf{z}_t \rangle] + \frac{4L_g + 5L_g \beta_1^2}{2(1 - \beta_1)^2} \sum_{t=1}^T \mathbb{E} [\|\mathbf{x}_{t+1} - \mathbf{x}_t\|^2]
\end{aligned}$$

□

Lemma 2.3 Assume $\|\hat{\mathbf{g}}_t\|_\infty \leq G_{zo}$, $\forall t \in [T]$ and $m_0 = 0$, By ZO-AdaMM update rule, we have

$$\begin{aligned}
\sum_{t=1}^T \mathbb{E}[\langle \nabla f_\mu(\mathbf{x}_t), \mathbf{z}_{t+1} - \mathbf{z}_t \rangle] & \leq \mathbb{E} \left[\left(\frac{\eta G_{zo}}{1 - \beta_1} + \eta^2 \right) \sum_{i=1}^d \frac{\alpha_1}{\sqrt{\hat{\mathbf{v}}_{0,i}}} \right] \\
& \quad - \sum_{t=1}^T \mathbb{E} \left[\langle \nabla f_\mu(\mathbf{x}_t), \alpha_t \hat{\mathbf{V}}_t^{-1/2} \nabla f_\mu(\mathbf{x}_t) \rangle \right]. \tag{33}
\end{aligned}$$

Proof of Lemma 2.3: By Lemma 2.1, we have

$$\begin{aligned}
& \langle \nabla f_\mu(\mathbf{x}_t), \mathbf{z}_{t+1} - \mathbf{z}_t \rangle \\
& = \langle \nabla f_\mu(\mathbf{x}_t), -\frac{\beta_1}{1 - \beta_1} \left(\alpha_t \hat{\mathbf{V}}_t^{-1/2} - \alpha_{t-1} \hat{\mathbf{V}}_{t-1}^{-1/2} \right) \mathbf{m}_{t-1} - \alpha_t \hat{\mathbf{V}}_t^{-1/2} \hat{\mathbf{g}}_t \rangle \\
& = \langle \nabla f_\mu(\mathbf{x}_t), -\frac{\beta_1}{1 - \beta_1} \left(\alpha_t \hat{\mathbf{V}}_t^{-1/2} - \alpha_{t-1} \hat{\mathbf{V}}_{t-1}^{-1/2} \right) \mathbf{m}_{t-1} \rangle - \langle \nabla f_\mu(\mathbf{x}_t), \alpha_t \hat{\mathbf{V}}_t^{-1/2} \hat{\mathbf{g}}_t \rangle, \tag{34}
\end{aligned}$$

and

$$\begin{aligned}
& \langle \nabla f_\mu(\mathbf{x}_t), \alpha_t \hat{\mathbf{V}}_t^{-1/2} \hat{\mathbf{g}}_t \rangle \\
&= \langle \nabla f_\mu(\mathbf{x}_t), \alpha_t \hat{\mathbf{V}}_t^{-1/2} \nabla f_\mu(\mathbf{x}_t) \rangle + \langle \nabla f_\mu(\mathbf{x}_t), \alpha_t \hat{\mathbf{V}}_t^{-1/2} (\hat{\mathbf{g}}_t - \nabla f_\mu(\mathbf{x}_t)) \rangle \\
&= \langle \nabla f_\mu(\mathbf{x}_t), \alpha_t \hat{\mathbf{V}}_t^{-1/2} \nabla f_\mu(\mathbf{x}_t) \rangle + \langle \nabla f_\mu(\mathbf{x}_t), \alpha_{t-1} \hat{\mathbf{V}}_{t-1}^{-1/2} (\hat{\mathbf{g}}_t - \nabla f_\mu(\mathbf{x}_t)) \rangle \\
&\quad + \langle \nabla f_\mu(\mathbf{x}_t), (\alpha_t \hat{\mathbf{V}}_t^{-1/2} - \alpha_{t-1} \hat{\mathbf{V}}_{t-1}^{-1/2}) (\hat{\mathbf{g}}_t - \nabla f_\mu(\mathbf{x}_t)) \rangle. \tag{35}
\end{aligned}$$

Substitute (35) into (34), we have

$$\begin{aligned}
& \langle \nabla f_\mu(\mathbf{x}_t), \mathbf{z}_{t+1} - \mathbf{z}_t \rangle \\
&\leq \langle \nabla f_\mu(\mathbf{x}_t), -\frac{\beta_1}{1-\beta_1} (\alpha_t \hat{\mathbf{V}}_t^{-1/2} - \alpha_{t-1} \hat{\mathbf{V}}_{t-1}^{-1/2}) \odot \mathbf{m}_{t-1} \rangle \\
&\quad - \langle \nabla f_\mu(\mathbf{x}_t), \alpha_t \hat{\mathbf{V}}_t^{-1/2} \nabla f_\mu(\mathbf{x}_t) \rangle - \langle \nabla f_\mu(\mathbf{x}_t), \alpha_{t-1} \hat{\mathbf{V}}_{t-1}^{-1/2} (\hat{\mathbf{g}}_t - \nabla f_\mu(\mathbf{x}_t)) \rangle \\
&\quad - \langle \nabla f_\mu(\mathbf{x}_t), (\alpha_t \hat{\mathbf{V}}_t^{-1/2} - \alpha_{t-1} \hat{\mathbf{V}}_{t-1}^{-1/2}) (\hat{\mathbf{g}}_t - \nabla f_\mu(\mathbf{x}_t)) \rangle \\
&= \langle \nabla f_\mu(\mathbf{x}_t), -\left(\alpha_t \hat{\mathbf{V}}_t^{-1/2} - \alpha_{t-1} \hat{\mathbf{V}}_{t-1}^{-1/2}\right) \frac{\mathbf{m}_t}{1-\beta_1} \rangle \\
&\quad - \langle \nabla f_\mu(\mathbf{x}_t), -\left(\alpha_t \hat{\mathbf{V}}_t^{-1/2} - \alpha_{t-1} \hat{\mathbf{V}}_{t-1}^{-1/2}\right) \nabla f_\mu(\mathbf{x}_t) \rangle \\
&\quad - \langle \nabla f_\mu(\mathbf{x}_t), \alpha_t \hat{\mathbf{V}}_t^{-1/2} \nabla f_\mu(\mathbf{x}_t) \rangle - \langle \nabla f_\mu(\mathbf{x}_t), \alpha_{t-1} \hat{\mathbf{V}}_{t-1}^{-1/2} (\hat{\mathbf{g}}_t - \nabla f_\mu(\mathbf{x}_t)) \rangle \\
&\leq \left(\frac{\eta G_{zo}}{1-\beta_1} + \eta^2\right) \sum_{i=1}^d \left| \frac{\alpha_{t-1}}{\sqrt{\hat{\mathbf{v}}_{t-1,i}}} - \frac{\alpha_t}{\sqrt{\hat{\mathbf{v}}_{t,i}}} \right| \\
&\quad - \langle \nabla f_\mu(\mathbf{x}_t), \alpha_t \hat{\mathbf{V}}_t^{-1/2} \nabla f_\mu(\mathbf{x}_t) \rangle - \langle \nabla f_\mu(\mathbf{x}_t), \alpha_{t-1} \hat{\mathbf{V}}_{t-1}^{-1/2} (\hat{\mathbf{g}}_t - \nabla f_\mu(\mathbf{x}_t)) \rangle \tag{36}
\end{aligned}$$

where the last inequality follows from the assumption that $\hat{\mathbf{V}}_t = \text{diga}(\hat{\mathbf{v}}_t)$, $\|\nabla f_\mu(\mathbf{x}_t)\|_\infty \leq \eta$ and $\|\hat{\mathbf{g}}_t\|_\infty \leq G_{zo}$.

The upper bound on $\|\mathbf{m}_t\|_\infty$ can be proved by a simple induction. Recall that $\mathbf{m}_t = \beta_{1,t} \mathbf{m}_{t-1} + (1 - \beta_{1,t}) \hat{\mathbf{g}}_t$, suppose $\|\mathbf{m}_{t-1}\|_\infty \leq G_{zo}$, we have

$$\begin{aligned}
\|\mathbf{m}_t\|_\infty &\leq (\beta_{1,t} + (1 - \beta_{1,t})) \max(\|\hat{\mathbf{g}}_t\|_\infty, \|\mathbf{m}_{t-1}\|_\infty) \\
&= \max(\|\hat{\mathbf{g}}_t\|_\infty, \|\mathbf{m}_{t-1}\|_\infty) \leq G_{zo}. \tag{37}
\end{aligned}$$

Then since $\mathbf{m}_0 = 0$, we have $\|\mathbf{m}_0\| \leq G_{zo}$, which completes the induction.

Sum t from 1 to T and take expectation over randomness of $\hat{\mathbf{g}}_t$, we have

$$\begin{aligned}
& \sum_{t=1}^T \mathbb{E}[\langle \nabla f_\mu(\mathbf{x}_t), \mathbf{z}_{t+1} - \mathbf{z}_t \rangle] \\
&\leq \mathbb{E} \left[\sum_{t=1}^T \left(\frac{\eta G_{zo}}{1-\beta_1} + \eta^2 \right) \sum_{i=1}^d \left| \frac{\alpha_{t-1}}{\sqrt{\hat{\mathbf{v}}_{t-1,i}}} - \frac{\alpha_t}{\sqrt{\hat{\mathbf{v}}_{t,i}}} \right| \right] \\
&\quad - \sum_{t=1}^T \mathbb{E} \left[\langle \nabla f_\mu(\mathbf{x}_t), \alpha_t \hat{\mathbf{V}}_t^{-1/2} \nabla f_\mu(\mathbf{x}_t) \rangle \right] - \sum_{t=1}^T \mathbb{E} \left[\langle \nabla f_\mu(\mathbf{x}_t), \alpha_{t-1} \hat{\mathbf{V}}_{t-1}^{-1/2} (\hat{\mathbf{g}}_t - \nabla f_\mu(\mathbf{x}_t)) \rangle \right] \\
&\leq \mathbb{E} \left[\left(\frac{\eta G_{zo}}{1-\beta_1} + \eta^2 \right) \sum_{i=1}^d \frac{\alpha_1}{\sqrt{\hat{\mathbf{v}}_{0,i}}} \right] - \sum_{t=1}^T \mathbb{E} \left[\langle \nabla f_\mu(\mathbf{x}_t), \alpha_t \hat{\mathbf{V}}_t^{-1/2} \nabla f_\mu(\mathbf{x}_t) \rangle \right]
\end{aligned}$$

where the last inequality follows from following facts.

1. Since $\hat{\mathbf{v}}_t = \max(\hat{\mathbf{v}}_{t-1}, \mathbf{v}_t)$, we know $\hat{\mathbf{v}}_t$ is non-decreasing. Given the fact that α_t is non-increasing (by our choice), we have $\alpha_{t-1}/\hat{\mathbf{v}}_{t-1,i} - \alpha_t/\hat{\mathbf{v}}_{t,i} \geq 0$. Thus, following inequality holds.

$$\begin{aligned} & \mathbb{E} \left[\sum_{t=1}^T \sum_{i=1}^d \left| \frac{\alpha_{t-1}}{\sqrt{\hat{\mathbf{v}}_{t-1,i}}} - \frac{\alpha_t}{\sqrt{\hat{\mathbf{v}}_{t,i}}} \right| \right] = \mathbb{E} \left[\sum_{i=1}^d \sum_{t=1}^T \left| \frac{\alpha_{t-1}}{\sqrt{\hat{\mathbf{v}}_{t-1,i}}} - \frac{\alpha_t}{\sqrt{\hat{\mathbf{v}}_{t,i}}} \right| \right] \\ & = \mathbb{E} \left[\sum_{i=1}^d \sum_{t=1}^T \left(\frac{\alpha_{t-1}}{\sqrt{\hat{\mathbf{v}}_{t-1,i}}} - \frac{\alpha_t}{\sqrt{\hat{\mathbf{v}}_{t,i}}} \right) \right] \leq \mathbb{E} \left[\sum_{i=1}^d \frac{\alpha_1}{\sqrt{\hat{\mathbf{v}}_{0,i}}} \right] \end{aligned} \quad (38)$$

2. We have $\mathbb{E}[\hat{\mathbf{g}}_t | \hat{\mathbf{g}}_{1:t-1}] = \nabla f_\mu(\mathbf{x}_t)$ by the assumption that $\mathbb{E}[\hat{\mathbf{g}}_t] = \nabla f_\mu(\mathbf{x}_t)$ and the noise on $\hat{\mathbf{g}}_t$ is independent of $\hat{\mathbf{g}}_{1:t-1}$. Thus, the following holds

$$\mathbb{E} \left[\langle \nabla f_\mu(\mathbf{x}_t), \alpha_{t-1} \hat{\mathbf{V}}_{t-1}^{-1/2} (\hat{\mathbf{g}}_t - \nabla f_\mu(\mathbf{x}_t)) \rangle \right] = 0 \quad (39)$$

□

Lemma 2.4 Assume $\gamma := \beta_1/\beta_2 < 1$, ZO-AdaMM yields

$$\|\mathbf{x}_{t+1} - \mathbf{x}_t\|^2 \leq \alpha_t^2 d \frac{1 - \beta_1}{1 - \beta_2} \frac{1}{1 - \gamma} \quad (40)$$

Comment: This is an important lemma for ZO-AdaMM, it shows the squared update quantity is not dependent on size of stochastic gradient, thus giving a tighter dependency on d compared with [18].

Proof of Lemma 2.4: By the update rule, we have

$$\begin{aligned} \|\mathbf{x}_{t+1} - \mathbf{x}_t\|^2 &= \alpha_t^2 \left\| \frac{\mathbf{m}_t}{\sqrt{\hat{\mathbf{v}}_t}} \right\|^2 \\ &\leq \alpha_t^2 \sum_{i=1}^d \frac{((1 - \beta_1) \sum_{j=0}^{t-1} \beta_1^{t-j} \hat{\mathbf{g}}_{j,i})^2}{(1 - \beta_2) \sum_{j=0}^{t-1} \beta_2^{t-j} \hat{\mathbf{g}}_{j,i}^2} \leq \alpha_t^2 \sum_{i=1}^d \frac{(1 - \beta_1)^2 (\sum_{j=0}^{t-1} \beta_1^{t-j}) (\sum_{j=0}^{t-1} \beta_1^{t-j} \hat{\mathbf{g}}_{j,i}^2)}{(1 - \beta_2) \sum_{j=0}^{t-1} \beta_2^{t-j} \hat{\mathbf{g}}_{j,i}^2} \\ &\leq \alpha_t^2 \sum_{i=1}^d \frac{(1 - \beta_1) \sum_{j=0}^{t-1} \beta_1^{t-j} \hat{\mathbf{g}}_{j,i}^2}{(1 - \beta_2) \sum_{j=0}^{t-1} \beta_2^{t-j} \hat{\mathbf{g}}_{j,i}^2} \leq \alpha_t^2 \sum_{i=1}^d \sum_{j=0}^{t-1} \frac{(1 - \beta_1) \beta_1^{t-j} \hat{\mathbf{g}}_{j,i}^2}{(1 - \beta_2) \beta_2^{t-j} \hat{\mathbf{g}}_{j,i}^2} \\ &\leq \alpha_t^2 d \sum_{j=0}^{t-1} \frac{1 - \beta_1}{1 - \beta_2} \gamma^{t-j} \leq \alpha_t^2 d \frac{1 - \beta_1}{1 - \beta_2} \frac{1}{1 - \gamma} \end{aligned}$$

where the second inequality is due to Cauchy-Schwarz and $\gamma = \beta_1/\beta_2 < 1$.

□

Proof of Proposition 2: Substitute (40) and (33) into (29), we get

$$\begin{aligned} & \mathbb{E}[f_\mu(\mathbf{z}_{t+1}) - f_\mu(\mathbf{z}_1)] \\ & \leq \sum_{t=1}^T \mathbb{E}[\langle \nabla f_\mu(\mathbf{x}_t), \mathbf{z}_{t+1} - \mathbf{z}_t \rangle] + \frac{4L_g + 5L_g\beta_1^2}{2(1 - \beta_1)^2} \sum_{t=1}^T \mathbb{E}[\|\mathbf{x}_{t+1} - \mathbf{x}_t\|^2] \\ & \leq \mathbb{E} \left[\left(\frac{\eta G_{zo}}{1 - \beta_1} + \eta^2 \right) \left\| \frac{\alpha_1}{\sqrt{\hat{\mathbf{v}}_0}} \right\|_1 \right] - \sum_{t=1}^T \mathbb{E} \left[\langle \nabla f_\mu(\mathbf{x}_t), \alpha_t \hat{\mathbf{V}}_t^{-1/2} \nabla f_\mu(\mathbf{x}_t) \rangle \right] \\ & \quad + \sum_{t=1}^T \alpha_t^2 d \frac{4L_g + 5L_g\beta_1^2}{2(1 - \beta_1)^2} \frac{1 - \beta_1}{1 - \beta_2} \frac{1}{1 - \gamma} \end{aligned} \quad (41)$$

Rearrange and assume $f_\mu(\mathbf{z}_1) - \min_{\mathbf{z}} f_\mu(\mathbf{z}) \leq D_f$, we get

$$\begin{aligned} & \sum_{t=1}^T \mathbb{E} \left[\langle \nabla f_\mu(\mathbf{x}_t), \alpha_t \hat{\mathbf{V}}_t^{-1/2} \nabla f_\mu(\mathbf{x}_t) \rangle \right] \\ & \leq D_f + \mathbb{E} \left[\left(\frac{\eta G_{zo}}{1 - \beta_1} + \eta^2 \right) \left\| \frac{\alpha_1}{\sqrt{\hat{\mathbf{v}}_0}} \right\|_1 \right] + \sum_{t=1}^T \alpha_t^2 d \frac{4L_g + 5L_g\beta_1^2}{2(1 - \beta_1)^2} \frac{1 - \beta_1}{1 - \beta_2} \frac{1}{1 - \gamma} \end{aligned} \quad (42)$$

Set $\alpha_t = \alpha = 1/\sqrt{Td}$ and divide both sides by $T\alpha$, uniformly randomly pick R from 1 to T ,

$$\begin{aligned} \mathbb{E} \left[\|\hat{\mathbf{V}}_R^{-1/2} \nabla f_\mu(x_R)\|^2 \right] &= \frac{1}{T} \sum_{t=1}^T \mathbb{E} \left[\|V_t^{-1/2} \nabla f_\mu(\mathbf{x}_t)\|^2 \right] \\ &\leq \frac{D_f}{T\alpha} + \frac{1}{T} \mathbb{E} \left[\left(\frac{\eta G_{zo}}{1-\beta_1} + \eta^2 \right) \left\| \frac{1}{\sqrt{\hat{\mathbf{v}}_0}} \right\|_1 \right] + \alpha d \frac{4L_g + 5L_g\beta_1^2}{2(1-\beta_1)^2} \frac{1-\beta_1}{1-\beta_2} \frac{1}{1-\gamma} \\ &= \frac{\sqrt{d}}{\sqrt{T}} D_f + \frac{1}{T} \mathbb{E} \left[\left(\frac{\eta G_{zo}}{1-\beta_1} + \eta^2 \right) \left\| \frac{1}{\sqrt{\hat{\mathbf{v}}_0}} \right\|_1 \right] + \frac{\sqrt{d}}{\sqrt{T}} \frac{4L_g + 5L_g\beta_1^2}{2(1-\beta_1)^2} \frac{1-\beta_1}{1-\beta_2} \frac{1}{1-\gamma} \end{aligned} \quad (43)$$

Since $\hat{\mathbf{V}}_{0,ii}^{1/2} \geq c$, $\forall i \in [d]$. By Lemma A1, we have

$$\|\hat{\mathbf{V}}_t^{-1/4} (\nabla f_\mu(x) - \nabla f_\mu(x))\|^2 \leq \frac{\mu^2 d^2 L^2}{4c} \quad (44)$$

Then we can easily adapt (43) to

$$\begin{aligned} \mathbb{E} \left[\|\hat{\mathbf{V}}_t^{-1/4} \nabla f(x_R)\|^2 \right] &\leq \frac{\mu^2 d^2 L^2}{2c} + 2 \frac{\sqrt{d}}{\sqrt{T}} D_f + 2 \frac{1}{T} \mathbb{E} \left[\left(\frac{\eta G_{zo}}{1-\beta_1} + 2\eta^2 \right) \left\| \frac{1}{\sqrt{\hat{\mathbf{v}}_0}} \right\|_1 \right] \\ &\quad + \frac{\sqrt{d}}{\sqrt{T}} \frac{4L_g + 5L_g\beta_1^2}{(1-\beta_1)^2} \frac{1-\beta_1}{1-\beta_2} \frac{1}{1-\gamma} \end{aligned}$$

Substituting into μ finishes the proof. \square

2.3 Proof of Proposition 3

Upon defining $G_{zo,i} := \max_{t \in [T]} |\hat{g}_{t,i}|$

by [50, Lemma 2.2], for a vector \mathbf{u} sampled from a unit sphere in \mathbb{R}^d , we have for any $i \in [d]$,

$$P[|u_i| \geq \sqrt{\xi/d}] \leq \exp((1-\xi + \log \xi)/2). \quad (45)$$

Let $\xi = 4 \log \frac{dT}{\delta}$, and by the assumption of $\max(d, T) \geq 3$ we have $1 + \log \xi \leq \xi/2$. Thus, we obtain from (45) that

$$P[|u_i| \geq \sqrt{\xi/d}] \leq \exp(-\xi/4) = \exp(-\log(dT/\delta)) = \delta/dT. \quad (46)$$

Recall that the ZO gradient estimate $\hat{\mathbf{g}}_t$ is given by the form

$$\hat{\nabla} f(\mathbf{x}) = (d/\mu)[f(\mathbf{x} + \mu\mathbf{u}) - f(\mathbf{x})]\mathbf{u}. \quad (47)$$

By Lipschitz of f under **A2**, the i th coordinate of the ZO gradient estimate (47) is upper bounded by $dL_c|u_i|$. Since \mathbf{u} is drawn uniformly randomly from a unit sphere, by (46) we have

$$P[dL_c|u_i| \geq L_c\sqrt{\xi d}] \leq \delta/dT. \quad (48)$$

Also, since $|\hat{g}_{t,i}| \leq dL_c|u_i|$, based on (48) we obtain that

$$P[|\hat{g}_{t,i}| \geq L_c\sqrt{\xi d}] \leq P[dL_c|u_i| \geq L_c\sqrt{\xi d}] \leq \delta/dT. \quad (49)$$

Substituting $\xi = 4 \log \frac{dT}{\delta}$ into (49), we have

$$P[|\hat{g}_{t,i}| \geq 2L_c\sqrt{d \log(dT/\delta)}] \leq \delta/dT \quad (50)$$

Then by the union bound and (50), we have

$$\begin{aligned} &P[|\hat{g}_{t,i}| \geq 2L_c\sqrt{d \log(dT/\delta)}, \forall i, t] \\ &\leq \sum_{t \in [T]} \sum_{i \in [d]} P[|\hat{g}_{t,i}| \geq 2L_c\sqrt{d \log(dT/\delta)}] \leq dT(\delta/dT) = \delta, \end{aligned}$$

which implies the inequality (11). \square

2.4 Proof of Theorem 1

The idea is to prove a similar result as Proposition 2 conditioned on the event in Proposition 3 ($\max_{t \in [T]} \{\|\hat{\mathbf{g}}_t\|_\infty\} \leq 2L_c\sqrt{d \log(dT/\delta)}$). Thus, the proof follows the same flow as Proposition 2. The difference is that (39) does not hold conditioned on the event and more efforts are need to bound

the corresponding term in (39). Denote the event that $\max_{t \in [T]} \{\|\hat{\mathbf{g}}_t\|_\infty\} \leq 2L_c \sqrt{d \log(dT/\delta)}$ to be $U(\delta)$, we need to upper bound

$$\mathbb{E} \left[\langle \nabla f_\mu(\mathbf{x}_t), \alpha_{t-1} \hat{\mathbf{V}}_{t-1}^{-1/2} (\hat{\mathbf{g}}_t - \nabla f_\mu(\mathbf{x}_t)) \rangle | U(\delta) \right] \quad (51)$$

where $\mathbb{E}[\cdot | U(\delta)]$ is conditional expectation conditioned on $U(\delta)$.

By Proposition 3, we know $P(U(\delta)) \geq 1 - \delta$ and using the fact that $E[\cdot | A] = \frac{E[\cdot] - E[\cdot | A^c]P(A^c)}{P(A)}$ for any event A and its complimentary event A^c , we have

$$\begin{aligned} & \mathbb{E} \left[\langle \nabla f_\mu(\mathbf{x}_t), \alpha_{t-1} \hat{\mathbf{V}}_{t-1}^{-1/2} (\hat{\mathbf{g}}_t - \nabla f_\mu(\mathbf{x}_t)) \rangle | U(\delta) \right] \\ & \leq \frac{\mathbb{E} \left[\langle \nabla f_\mu(\mathbf{x}_t), \alpha_{t-1} \hat{\mathbf{V}}_{t-1}^{-1/2} (\hat{\mathbf{g}}_t - \nabla f_\mu(\mathbf{x}_t)) \rangle \right]}{1 - \delta} \\ & \quad + \frac{\delta \left| \mathbb{E} \left[\langle \nabla f_\mu(\mathbf{x}_t), \alpha_{t-1} \hat{\mathbf{V}}_{t-1}^{-1/2} (\hat{\mathbf{g}}_t - \nabla f_\mu(\mathbf{x}_t)) \rangle | U(\delta)^c \right] \right|}{1 - \delta} \end{aligned} \quad (52)$$

and further we have

$$\begin{aligned} & \left| \mathbb{E} \left[\langle \nabla f_\mu(\mathbf{x}_t), \alpha_{t-1} \hat{\mathbf{V}}_{t-1}^{-1/2} (\hat{\mathbf{g}}_t - \nabla f_\mu(\mathbf{x}_t)) \rangle | U(\delta)^c \right] \right| \\ & \leq d \frac{\alpha_{t-1}}{c} (\eta^2 + \eta \max_{t \in [T]} \|\hat{\mathbf{g}}_t\|_\infty) \\ & \leq d \frac{\alpha_{t-1}}{c} (\eta^2 + \eta d L_c) \end{aligned} \quad (53)$$

where the first inequality is due to $\|\nabla f_\mu(x_t)\|_\infty \leq \eta$ and $\hat{v}_{t-1}^{1/2} \geq \hat{v}_0^{1/2} \geq c\mathbf{1}$, the second inequality is due to (1) and Lipschitz continuity of $f(\mathbf{x}; \boldsymbol{\xi})$.

Using the fact that $\mathbb{E} \left[\langle \nabla f_\mu(\mathbf{x}_t), \alpha_{t-1} \hat{\mathbf{V}}_{t-1}^{-1/2} (\hat{\mathbf{g}}_t - \nabla f_\mu(\mathbf{x}_t)) \rangle \right] = 0$ proved in in (39) and set $\delta = 1/Td^{0.5}$, we have for $T \geq 2$

$$\begin{aligned} & \mathbb{E} \left[\langle \nabla f_\mu(\mathbf{x}_t), \alpha_{t-1} \hat{\mathbf{V}}_{t-1}^{-1/2} (\hat{\mathbf{g}}_t - \nabla f_\mu(\mathbf{x}_t)) \rangle | U(1/Td^{0.5}) \right] \\ & \leq 2 \frac{1}{Td^{0.5}} d \frac{\alpha_{t-1}}{c} (\eta^2 + \eta d L_c) = 2 \frac{d^{1.5}}{T} \frac{\alpha_{t-1}}{c} \eta L_c + 2 \frac{d^{0.5}}{T} \frac{\alpha_{t-1}}{c} \eta^2 \end{aligned} \quad (54)$$

Replacing (39) with (54) and going through the rest of the proof of Proposition (2), one can finally get

$$\begin{aligned} & \mathbb{E} \left[\|\hat{\mathbf{V}}_t^{-1/4} \nabla f(x_R)\|^2 | U(1/Td^{0.5}) \right] \\ & \leq \frac{\mu^2 d^2 L^2}{2c} + 2 \frac{\sqrt{d}}{\sqrt{T}} D_f + 2 \frac{1}{T} \mathbb{E} \left[\left(\frac{\eta G_{z_0}}{1 - \beta_1} + 2\eta^2 \right) \left\| \frac{1}{\sqrt{\hat{\mathbf{v}}_0}} \right\|_1 \right] | U(1/Td^{0.5}) \\ & \quad + \frac{\sqrt{d}}{\sqrt{T}} \frac{4L_g + 5L_g \beta_1^2}{(1 - \beta_1)^2} \frac{1 - \beta_1}{1 - \beta_2} \frac{1}{1 - \gamma} + 2 \frac{d^{1.5}}{T} \frac{\eta L_c}{c} + 2 \frac{d^{0.5}}{T} \frac{\eta^2}{c}. \end{aligned}$$

Since in the event of $U(1/Td^{0.5})$, we have

$$G_{z_0} = \max_{t \in [T]} \{\|\hat{\mathbf{g}}_t\|_\infty\} \leq 2L_c \sqrt{d \log(d^{1.5} T^2)} = 2L_c \sqrt{d} \sqrt{1.5 \log d + 2 \log T}. \quad (55)$$

Substituting the above inequality into (55), we get the desired result. \square

2.5 Proof of Theorem 2

To proceed into proof of Theorem 2, we give a few technical lemmas for the properties of (7).

Lemma 2.5 *For any symmetric $\mathbf{H} \succeq 0$, \mathbf{g}, ω , we have*

$$\langle \mathbf{g}, P_{\mathcal{X}, \mathbf{H}}(\mathbf{x}^-, \mathbf{g}, \omega) \rangle \geq \|\mathbf{H}^{1/2} P_{\mathcal{X}, \mathbf{H}}(\mathbf{x}^-, \mathbf{g}, \omega)\|^2 \quad (56)$$

Proof of Lemma 2.5: By definition of \mathbf{x}^+ , the optimality condition of (6) is

$$\langle \mathbf{g} + \frac{1}{\omega} \mathbf{H}(\mathbf{x}^+ - \mathbf{x}^-), \mathbf{x} - \mathbf{x}^+ \rangle \geq 0 \quad \forall \mathbf{x} \in \mathcal{X}$$

Thus

$$\langle \mathbf{g} + \frac{1}{\omega} \mathbf{H}(\mathbf{x}^+ - x), \mathbf{x} - \mathbf{x}^+ \rangle \geq 0$$

which can be rearranged to

$$\langle \mathbf{g}, P_{\mathcal{X}, \mathbf{H}}(\mathbf{x}^-, \mathbf{g}, \omega) \rangle = \frac{1}{\omega} \langle \mathbf{g}, x - \mathbf{x}^+ \rangle \geq \frac{1}{\omega^2} \langle \mathbf{H}(x - \mathbf{x}^+), x - \mathbf{x}^+ \rangle = \|\mathbf{H}^{1/2} P_{\mathcal{X}, \mathbf{H}}(\mathbf{x}^-, \mathbf{g}, \omega)\|^2$$

This completes the proof. \square

Lemma 2.6 Let \mathbf{x}_1^+ and \mathbf{x}_2^+ be given by (6) with \mathbf{g} replaced by \mathbf{g}_1 and \mathbf{g}_2 , with $H \succ 0$, we have

$$\|\mathbf{x}_1^+ - \mathbf{x}_2^+\| \leq \frac{\omega}{\lambda_{\min}(\mathbf{H})} \|\mathbf{g}_1 - \mathbf{g}_2\| \quad (57)$$

$$\|\mathbf{H}^{1/2}(\mathbf{x}_1^+ - \mathbf{x}_2^+)\| \leq \omega \|\mathbf{H}^{-1/2}(\mathbf{g}_1 - \mathbf{g}_2)\|. \quad (58)$$

where $\lambda_{\min}(\mathbf{H})$ is the minimum eigenvalue of \mathbf{H} .

Proof of Lemma 2.6: By definition of \mathbf{x}^+ , the optimality condition of (6) is

$$\langle \mathbf{g} + \frac{1}{\omega} \mathbf{H}(\mathbf{x}^+ - \mathbf{x}^-), \mathbf{x} - \mathbf{x}^+ \rangle \geq 0 \quad \forall \mathbf{x} \in \mathcal{X}$$

Thus, we have

$$\langle \mathbf{g}_1 + \frac{1}{\omega} \mathbf{H}(\mathbf{x}_1^+ - \mathbf{x}^-, \mathbf{x}_2^+ - \mathbf{x}_1^+) \rangle \geq 0$$

$$\langle \mathbf{g}_2 + \frac{1}{\omega} \mathbf{H}(\mathbf{x}_2^+ - \mathbf{x}^-, \mathbf{x}_1^+ - \mathbf{x}_2^+) \rangle \geq 0$$

Summing up the above two inequalities, we get

$$\langle \mathbf{g}_1 - \mathbf{g}_2, \mathbf{x}_2^+ - \mathbf{x}_1^+ \rangle \geq \frac{1}{\omega} \langle \mathbf{H}(\mathbf{x}_2^+ - \mathbf{x}_1^+), \mathbf{x}_2^+ - \mathbf{x}_1^+ \rangle \quad (59)$$

By Cauchy-Schwarz inequality, we get

$$\begin{aligned} \|\mathbf{g}_1 - \mathbf{g}_2\| \|\mathbf{x}_2^+ - \mathbf{x}_1^+\| &\geq \langle \mathbf{g}_1 - \mathbf{g}_2, \mathbf{x}_2^+ - \mathbf{x}_1^+ \rangle \geq \frac{1}{\omega} \langle \mathbf{H}(\mathbf{x}_2^+ - \mathbf{x}_1^+), \mathbf{x}_2^+ - \mathbf{x}_1^+ \rangle \\ &\geq \frac{1}{\omega} \lambda_{\min}(\mathbf{H}) \|\mathbf{x}_2^+ - \mathbf{x}_1^+\|^2 \end{aligned}$$

which gives (57).

Further, by (59) and Cauchy-Schwarz, we also have

$$\begin{aligned} \|\mathbf{H}^{-1/2}(\mathbf{g}_1 - \mathbf{g}_2)\| \|\mathbf{H}^{1/2}(\mathbf{x}_2^+ - \mathbf{x}_1^+)\| &\geq \langle \mathbf{g}_1 - \mathbf{g}_2, \mathbf{x}_2^+ - \mathbf{x}_1^+ \rangle \\ &\geq \frac{1}{\omega} \langle \mathbf{H}(\mathbf{x}_2^+ - \mathbf{x}_1^+), \mathbf{x}_2^+ - \mathbf{x}_1^+ \rangle = \frac{1}{\omega} \|\mathbf{H}^{1/2}(\mathbf{x}_2^+ - \mathbf{x}_1^+)\|^2 \end{aligned}$$

which gives (58). This completes the proof. \square

The following lemma characterizes the difference between projected points if different distance matrices are used in ZO-AdaMM.

Lemma 2.7 Assume $\mathbf{V}_t^{1/2} \geq c\mathbf{I}$, ZO-AdaMM yields

$$\left\| (P_{\mathcal{X}, \hat{\mathbf{V}}_{t-1}^{1/2}}(\mathbf{x}_t, \nabla f_\mu(\mathbf{x}_t), \alpha_t) - P_{\mathcal{X}, \hat{\mathbf{V}}_t^{1/2}}(\mathbf{x}_t, \nabla f_\mu(\mathbf{x}_t), \alpha_t)) \right\|^2 \leq \sum_{i=1}^d v_{t,i}^{1/2} (\hat{v}_{t,i}^{1/2} - \hat{v}_{t-1,i}^{1/2}) \frac{1}{c^4} \eta^2. \quad (60)$$

Proof of Lemma 2.7: Recall the optimality condition of (6) is

$$\langle \mathbf{g} + \frac{1}{\omega} \mathbf{H}(\mathbf{x}^+ - \mathbf{x}^-, \mathbf{x} - \mathbf{x}^+) \rangle \geq 0 \quad \forall \mathbf{x} \in \mathcal{X} \quad (61)$$

Let us define

$$\begin{aligned}\mathbf{x}_t^* &\triangleq \mathbf{x}_t - \alpha_t P_{\mathcal{X}, \hat{\mathbf{V}}_t^{1/2}}(\mathbf{x}_t, \nabla f_\mu(\mathbf{x}_t), \alpha_t) \\ \tilde{\mathbf{x}}_t^* &\triangleq \mathbf{x}_t - \alpha_t P_{\mathcal{X}, \hat{\mathbf{V}}_t^{1/2}}(\mathbf{x}_t, \nabla f_\mu(\mathbf{x}_t), \alpha_t).\end{aligned}$$

By optimality condition (61), we have

$$\begin{aligned}\langle \nabla f_\mu(\mathbf{x}_t) + \frac{1}{\alpha_t} \hat{\mathbf{V}}_t^{1/2}(\tilde{\mathbf{x}}_t^* - \mathbf{x}_t), \mathbf{x}_t^* - \tilde{\mathbf{x}}_t^* \rangle &\geq 0 \\ \langle \nabla f_\mu(\mathbf{x}_t) + \frac{1}{\alpha_t} \hat{\mathbf{V}}_{t-1}^{1/2}(\mathbf{x}_t^* - \mathbf{x}_t), \tilde{\mathbf{x}}_t^* - \mathbf{x}_t^* \rangle &\geq 0\end{aligned}$$

Summing the above up, we get

$$\langle \hat{\mathbf{V}}_t^{1/2}(\tilde{\mathbf{x}}_t^* - \mathbf{x}_t) - \hat{\mathbf{V}}_{t-1}^{1/2}(\mathbf{x}_t^* - \mathbf{x}_t), \mathbf{x}_t^* - \tilde{\mathbf{x}}_t^* \rangle \geq 0$$

which is equivalent to

$$\begin{aligned}\langle (\hat{\mathbf{V}}_t^{1/2} - \hat{\mathbf{V}}_{t-1}^{1/2})(\mathbf{x}_t^* - \mathbf{x}_t), \mathbf{x}_t^* - \tilde{\mathbf{x}}_t^* \rangle \\ + \langle \hat{\mathbf{V}}_t^{1/2}(\tilde{\mathbf{x}}_t^* - \mathbf{x}_t^*), \mathbf{x}_t^* - \tilde{\mathbf{x}}_t^* \rangle \geq 0.\end{aligned}$$

Further rearranging, we have

$$\langle (\hat{\mathbf{V}}_t^{1/2} - \hat{\mathbf{V}}_{t-1}^{1/2})(\mathbf{x}_t^* - \mathbf{x}_t), \mathbf{x}_t^* - \tilde{\mathbf{x}}_t^* \rangle \geq \|\hat{\mathbf{V}}_t^{1/4}(\tilde{\mathbf{x}}_t^* - \mathbf{x}_t^*)\|^2 \geq c\|\tilde{\mathbf{x}}_t^* - \mathbf{x}_t^*\|^2$$

which implies (by using Cauchy-Swartz on the left hand side and then squaring both sides)

$$\begin{aligned}c^2\|\tilde{\mathbf{x}}_t^* - \mathbf{x}_t^*\|^2 &\leq \|(\hat{\mathbf{V}}_t^{1/2} - \hat{\mathbf{V}}_{t-1}^{1/2})(\mathbf{x}_t^* - \mathbf{x}_t)\|^2 = \sum_{i=1}^d (\hat{v}_{t,i}^{1/2} - \hat{v}_{t-1,i}^{1/2})^2 (\hat{x}_{t,i}^* - x_{t,i})^2 \\ &\stackrel{(a)}{\leq} \sum_{i=1}^d \hat{v}_{t,i}^{1/2} (\hat{v}_{t,i}^{1/2} - \hat{v}_{t-1,i}^{1/2}) \|\hat{x}_t^* - x_t\|^2 \stackrel{(b)}{\leq} \sum_{i=1}^d \hat{v}_{t,i}^{1/2} (\hat{v}_{t,i}^{1/2} - \hat{v}_{t-1,i}^{1/2}) \frac{1}{c^2} \alpha_t^2 \|\nabla f_\mu(x_t)\|^2 \\ &\leq \sum_{i=1}^d \hat{v}_{t,i}^{1/2} (\hat{v}_{t,i}^{1/2} - \hat{v}_{t-1,i}^{1/2}) \frac{1}{c^2} \alpha_t^2 \eta^2\end{aligned}\tag{62}$$

where (a) is due to $\hat{v}_{t,i}^{1/2} \geq \hat{v}_{t-1,i}^{1/2}$ and (b) is due to Lemma 2.6 by treating $\mathbf{g}_1 = \nabla f_\mu(\mathbf{x}_t)$, $\mathbf{g}_2 = 0$, $\mathbf{x}^- = \mathbf{x}_t$, $H = \hat{\mathbf{V}}_t^{1/2}$. Substituting (7) into LHS of the above inequality and rearrange, we get (60). This completes the proof. \square

Now we are ready to prove our main theorem.

Proof of Theorem 2:

We start with standard decent lemma in nonconvex optimization. By Lipschitz smoothness of f_μ , we have

$$f_\mu(\mathbf{x}_{t+1}) \leq f_\mu(\mathbf{x}_t) - \alpha_t \langle \nabla f_\mu(\mathbf{x}_t), P_{\mathcal{X}, \hat{\mathbf{V}}_t^{1/2}}(\mathbf{x}_t, \hat{\mathbf{g}}_t, \alpha_t) \rangle + \frac{L}{2} \alpha_t^2 \|P_{\mathcal{X}, \hat{\mathbf{V}}_t^{1/2}}(\mathbf{x}_t, \hat{\mathbf{g}}_t, \alpha_t)\|^2.\tag{63}$$

We need to upper bound RHS of the above inequality and split out a descent quantity.

$$\begin{aligned}& - \langle \nabla f_\mu(\mathbf{x}_t), P_{\mathcal{X}, \hat{\mathbf{V}}_t^{1/2}}(\mathbf{x}_t, \hat{\mathbf{g}}_t, \alpha_t) \rangle \\ &= - \langle \hat{\mathbf{g}}_t, P_{\mathcal{X}, \hat{\mathbf{V}}_t^{1/2}}(\mathbf{x}_t, \hat{\mathbf{g}}_t, \alpha_t) \rangle + \langle \hat{\mathbf{g}}_t - \nabla f_\mu(\mathbf{x}_t), P_{\mathcal{X}, \hat{\mathbf{V}}_t^{1/2}}(\mathbf{x}_t, \hat{\mathbf{g}}_t, \alpha_t) \rangle \\ &\leq - \|\hat{\mathbf{V}}_t^{1/4} P_{\mathcal{X}, \hat{\mathbf{V}}_t^{1/2}}(\mathbf{x}_t, \hat{\mathbf{g}}_t, \alpha_t)\|^2 + \langle \hat{\mathbf{g}}_t - \nabla f_\mu(\mathbf{x}_t), P_{\mathcal{X}, \hat{\mathbf{V}}_t^{1/2}}(\mathbf{x}_t, \hat{\mathbf{g}}_t, \alpha_t) \rangle\end{aligned}\tag{64}$$

where the inequality is by Lemma (2.5) and some simple substitutions.

Further, for the last term in RHS of (64) we have

$$\begin{aligned}
& \langle \hat{\mathbf{g}}_t - \nabla f_\mu(\mathbf{x}_t), P_{\mathcal{X}, \hat{\mathbf{V}}_t^{1/2}}(\mathbf{x}_t, \hat{\mathbf{g}}_t, \alpha_t) \rangle \\
&= \left. \begin{aligned}
& + \langle \hat{\mathbf{g}}_t - \nabla f_\mu(\mathbf{x}_t), P_{\mathcal{X}, \hat{\mathbf{V}}_t^{1/2}}(\mathbf{x}_t, \hat{\mathbf{g}}_t, \alpha_t) \rangle \\
& - \langle \hat{\mathbf{g}}_t - \nabla f_\mu(\mathbf{x}_t), P_{\mathcal{X}, \hat{\mathbf{V}}_t^{1/2}}(\mathbf{x}_t, \nabla f_\mu(\mathbf{x}_t), \alpha_t) \rangle \end{aligned} \right\} A \\
&+ \left. \begin{aligned}
& + \langle \hat{\mathbf{g}}_t - \nabla f_\mu(\mathbf{x}_t), P_{\mathcal{X}, \hat{\mathbf{V}}_t^{1/2}}(\mathbf{x}_t, \nabla f_\mu(\mathbf{x}_t), \alpha_t) \rangle \\
& - \langle \hat{\mathbf{g}}_t - \nabla f_\mu(\mathbf{x}_t), P_{\mathcal{X}, \hat{\mathbf{V}}_{t-1}^{1/2}}(\mathbf{x}_t, \nabla f_\mu(\mathbf{x}_t), \alpha_t) \rangle \end{aligned} \right\} B \\
&+ \underbrace{\langle \hat{\mathbf{g}}_t - \nabla f_\mu(\mathbf{x}_t), P_{\mathcal{X}, \hat{\mathbf{V}}_{t-1}^{1/2}}(\mathbf{x}_t, \nabla f_\mu(\mathbf{x}_t), \alpha_t) \rangle}_C
\end{aligned} \tag{65}$$

Next, we bound the three terms in RHS of (65).

Let's bound term A first, with the assumption $\hat{\mathbf{V}}^{1/2} \geq c\mathbf{I}$, by Lemma 2.6, (7) and Cauchy-Schwartz inequality, we have:

$$A = \langle \hat{\mathbf{g}}_t - \nabla f_\mu(\mathbf{x}_t), P_{\mathcal{X}, \hat{\mathbf{V}}_t^{1/2}}(\mathbf{x}_t, \hat{\mathbf{g}}_t, \alpha_t) - P_{\mathcal{X}, \hat{\mathbf{V}}_t^{1/2}}(\mathbf{x}_t, \nabla f_\mu(\mathbf{x}_t), \alpha_t) \rangle \leq \frac{1}{c} \|\hat{\mathbf{g}}_t - \nabla f_\mu(\mathbf{x}_t)\|^2 \tag{66}$$

Now let's bound term C , because $\mathbb{E}[\hat{\mathbf{g}}_t] = \nabla f_\mu(\mathbf{x}_t)$ and the noise in $\hat{\mathbf{g}}_t$ is independent of $\nabla f_\mu(\mathbf{x}_t)$ and $\hat{\mathbf{V}}_{t-1}$, we have

$$\mathbb{E}[\langle \nabla f_\mu(\mathbf{x}_t) - \hat{\mathbf{g}}_t, P_{\mathcal{X}, \hat{\mathbf{V}}_{t-1}^{1/2}}(\mathbf{x}_t, \nabla f_\mu(\mathbf{x}_t), \alpha_t) \rangle] = 0 \tag{67}$$

Substituting the above bounds for A and C , into (65) and (64), using Young's inequality on term B , we have

$$\begin{aligned}
& - \mathbb{E}[\langle \nabla f_\mu(\mathbf{x}_t), P_{\mathcal{X}, \hat{\mathbf{V}}_t^{1/2}}(\mathbf{x}_t, \hat{\mathbf{g}}_t, \alpha_t) \rangle] \\
& \leq - \mathbb{E}[\|\hat{\mathbf{V}}_t^{1/4} P_{\mathcal{X}, \hat{\mathbf{V}}_t^{1/2}}(\mathbf{x}_t, \hat{\mathbf{g}}_t, \alpha_t)\|^2] + \frac{1}{c} \mathbb{E}[\|\hat{\mathbf{g}}_t - \nabla f_\mu(\mathbf{x}_t)\|^2] + \frac{1}{2} \mathbb{E}[\|\hat{\mathbf{g}}_t - \nabla f_\mu(\mathbf{x}_t)\|^2] + \frac{1}{2} \mathbb{E}[B_2]
\end{aligned} \tag{68}$$

where we define

$$B_2 := \left\| (P_{\mathcal{X}, \hat{\mathbf{V}}_{t-1}^{1/2}}(\mathbf{x}_t, \nabla f_\mu(\mathbf{x}_t), \alpha_t) - P_{\mathcal{X}, \hat{\mathbf{V}}_t^{1/2}}(\mathbf{x}_t, \nabla f_\mu(\mathbf{x}_t), \alpha_t)) \right\|^2.$$

What remains is to bound the term B_2 which is given by Lemma 2.7.

Combining (63), (68), (60), we have

$$\begin{aligned}
\mathbb{E}[f_\mu(\mathbf{x}_{t+1})] & \leq \mathbb{E}[f_\mu(\mathbf{x}_t)] - \alpha_t \mathbb{E}[\|\hat{\mathbf{V}}_t^{1/4} P_{\mathcal{X}, \hat{\mathbf{V}}_t^{1/2}}(\mathbf{x}_t, \hat{\mathbf{g}}_t, \alpha_t)\|^2] + \alpha_t \left(\frac{1}{c} + \frac{1}{2}\right) \mathbb{E}[\|\hat{\mathbf{g}}_t - \nabla f_\mu(\mathbf{x}_t)\|^2] \\
& + \alpha_t \frac{1}{2} \mathbb{E} \left[\sum_{i=1}^d \hat{v}_{t,i}^{1/2} (\hat{v}_{t,i}^{1/2} - \hat{v}_{t-1,i}^{1/2}) \frac{1}{c^4} \eta^2 \right] + \frac{L}{2} \alpha_t^2 \mathbb{E} \left[\frac{1}{c^2} \|\hat{\mathbf{V}}_t^{1/4} P_{\mathcal{X}, \hat{\mathbf{V}}_t^{1/2}}(\mathbf{x}_t, \hat{\mathbf{g}}_t, \alpha_t)\|^2 \right]
\end{aligned} \tag{69}$$

which can be rearranged into

$$\begin{aligned}
& \left(\alpha_t - \frac{L}{2c^2} \alpha_t^2\right) \mathbb{E}[\|\hat{\mathbf{V}}_t^{1/4} P_{\mathcal{X}, \hat{\mathbf{V}}_t^{1/2}}(\mathbf{x}_t, \hat{\mathbf{g}}_t, \alpha_t)\|^2] \\
& \leq \mathbb{E}[f_\mu(\mathbf{x}_t)] - \mathbb{E}[f_\mu(\mathbf{x}_{t+1})] + \alpha_t \left(\frac{1}{c} + \frac{1}{2}\right) \mathbb{E}[\|\hat{\mathbf{g}}_t - \nabla f_\mu(\mathbf{x}_t)\|^2] \\
& + \alpha_t \frac{1}{2} \mathbb{E} \left[\sum_{i=1}^d \hat{v}_{t,i}^{1/2} (\hat{v}_{t,i}^{1/2} - \hat{v}_{t-1,i}^{1/2}) \frac{1}{c^4} \eta^2 \right].
\end{aligned} \tag{70}$$

In addition, we have

$$\begin{aligned}
& \|\hat{\mathbf{V}}_t^{1/4} P_{\mathcal{X}, \hat{\mathbf{V}}_t^{1/2}}(\mathbf{x}_t, \nabla f(\mathbf{x}_t), \alpha_t)\|^2 \leq 3 \|\hat{\mathbf{V}}_t^{1/4} P_{\mathcal{X}, \hat{\mathbf{V}}_t^{1/2}}(\mathbf{x}_t, \hat{\mathbf{g}}_t, \alpha_t)\|^2 \\
& \quad + 3 \|\hat{\mathbf{V}}_t^{1/4} (P_{\mathcal{X}, \hat{\mathbf{V}}_t^{1/2}}(\mathbf{x}_t, \nabla f_\mu(\mathbf{x}_t), \alpha_t) - P_{\mathcal{X}, \hat{\mathbf{V}}_t^{1/2}}(\mathbf{x}_t, \nabla f(\mathbf{x}_t), \alpha_t))\|^2 \\
& \quad + 3 \|\hat{\mathbf{V}}_t^{1/4} (P_{\mathcal{X}, \hat{\mathbf{V}}_t^{1/2}}(\mathbf{x}_t, \hat{\mathbf{g}}_t, \alpha_t) - P_{\mathcal{X}, \hat{\mathbf{V}}_t^{1/2}}(\mathbf{x}_t, \nabla f_\mu(\mathbf{x}_t), \alpha_t))\|^2 \\
& \leq 3 \|\hat{\mathbf{V}}_t^{1/4} P_{\mathcal{X}, \hat{\mathbf{V}}_t^{1/2}}(\mathbf{x}_t, \hat{\mathbf{g}}_t, \alpha_t)\|^2 + \frac{3}{c} \|\nabla f_\mu(\mathbf{x}_t) - \nabla f(\mathbf{x}_t)\|^2 + \frac{3}{c} \|\hat{\mathbf{g}}_t - \nabla f_\mu(\mathbf{x}_t)\|^2 \tag{71}
\end{aligned}$$

where the second inequality is by (7) and Lemma (2.6)

Combining (71) and (70), we have

$$\begin{aligned}
& \left(\alpha_t - \frac{L}{2c^2} \alpha_t^2 \right) \|\hat{\mathbf{V}}_t^{1/4} P_{\mathcal{X}, \hat{\mathbf{V}}_t^{1/2}}(\mathbf{x}_t, \nabla f(\mathbf{x}_t), \alpha_t)\|^2 \\
& \leq 3(\mathbb{E}[f_\mu(\mathbf{x}_t)] - \mathbb{E}[f_\mu(\mathbf{x}_{t+1})]) + (3\alpha_t(\frac{1}{c} + \frac{1}{2}) + \frac{3}{c}(\alpha_t - \frac{L}{2c^2} \alpha_t^2)) \mathbb{E}[\|\hat{\mathbf{g}}_t - f_\mu(\mathbf{x}_t)\|^2] \\
& \quad + \frac{3}{2} \alpha_t \mathbb{E}[\sum_{i=1}^d \hat{v}_{t,i}^{1/2} (\hat{v}_{t,i}^{1/2} - \hat{v}_{t-1,i}^{1/2}) \frac{1}{c^4} \eta^2] + \frac{3}{c} (\alpha_t - \frac{L}{2c^2} \alpha_t^2) \|\nabla f_\mu(\mathbf{x}_t) - \nabla f(\mathbf{x}_t)\|^2 \tag{72}
\end{aligned}$$

Summing over t from 1 to T , setting $\alpha_t = \alpha$, and dividing both sides by $T(\alpha - \frac{L_g \alpha^2}{2c^2})$, we get

$$\begin{aligned}
& \frac{1}{T} \sum_{t=1}^T \mathbb{E}[\|\hat{\mathbf{V}}_t^{1/4} P_{\mathcal{X}, \hat{\mathbf{V}}_t^{1/2}}(\mathbf{x}_t, \nabla f(\mathbf{x}_t), \alpha_t)\|^2] \\
& \leq \frac{3}{T(\alpha - \frac{L_g \alpha^2}{2c^2})} (\mathbb{E}[f_\mu(\mathbf{x}_1)] - \mathbb{E}[f_\mu(\mathbf{x}_{T+1})]) + \left(\frac{3\alpha(c+2)}{2Tc(\alpha - \frac{L_g \alpha^2}{2c^2})} + \frac{3}{Tc} \right) \sum_{t=1}^T \mathbb{E}[\|\hat{\mathbf{g}}_t - f_\mu(\mathbf{x}_t)\|^2] \\
& \quad + \frac{3\alpha}{2T(\alpha - \frac{L_g \alpha^2}{2c^2})} \mathbb{E}[\sum_{i=1}^d \hat{v}_{T,i}] \frac{1}{c^4} \eta^2 + \frac{3}{Tc} \sum_{t=1}^T \mathbb{E}[\|\nabla f_\mu(\mathbf{x}_t) - \nabla f(\mathbf{x}_t)\|^2]. \tag{73}
\end{aligned}$$

Choose $\alpha \leq \frac{c}{L}$, we have

$$\alpha - \frac{L_g \alpha^2}{2c} = \alpha \left(1 - \frac{L_g \alpha}{2c} \right) \geq \alpha \left(1 - \frac{1}{2} \right) = \frac{\alpha}{2} \tag{74}$$

and (73) becomes

$$\begin{aligned}
& \frac{1}{T} \sum_{t=1}^T \mathbb{E} \left[\|\hat{\mathbf{V}}_t^{1/4} P_{\mathcal{X}, \hat{\mathbf{V}}_t^{1/2}}(\mathbf{x}_t, \nabla f(\mathbf{x}_t), \alpha_t)\|^2 \right] \\
& \leq \frac{6}{T\alpha} D_f + \frac{1}{T} \left(\frac{9}{c} + 3 \right) \sum_{t=1}^T \mathbb{E} [\|\hat{\mathbf{g}}_t - f_\mu(\mathbf{x}_t)\|^2] + \frac{3}{T} \frac{1}{c^4} \eta^2 \mathbb{E} \left[\sum_{i=1}^d \hat{v}_{T,i} \right] + \frac{3}{c} \frac{\mu^2 d^2 L_g^2}{4} \tag{75}
\end{aligned}$$

where we defined $D_f := \mathbb{E}[f_\mu(\mathbf{x}_1)] - \min_x f_\mu(x)$ and used the fact that $\|\nabla f_\mu(\mathbf{x}_t) - \nabla f(\mathbf{x}_t)\|^2 \leq \frac{\mu^2 d^2 L_g^2}{4}$ by Lemma A1.

Further, we have

$$\begin{aligned}
& \mathbb{E} \left[\sum_{i=1}^d \hat{v}_{T,i} \right] = \mathbb{E} \left[\sum_{i=1}^d \max_{t \in [T]} (1 - \beta_2) \sum_{k=1}^t \beta_2^{t-k} \hat{g}_{k,i}^2 \right] \\
& \leq \mathbb{E} \left[d \max_{t \in [T]} (1 - \beta_2) \sum_{k=1}^t \beta_2^{t-k} \|\hat{g}_k\|_\infty \right] \\
& \leq \mathbb{E} \left[d \max_{t \in [T]} \|\hat{g}_t\|_\infty \right] \tag{76}
\end{aligned}$$

where the last inequality holds since $\sum_{k=1}^T \beta_2^{T-k} \leq 1/(1 - \beta_2)$.

Uniformly randomly picking R from 1 to T and substituting (76) into (75) finishes the proof. \square

3 Proof for Convex Optimization

3.1 Proof of Proposition 4

We follow the analytic framework in [18, Theorem 4] Based on Lemma A1, we obtain that $f_{t,\mu}$ defined in (2) (with respect to f_t) is convex. The convexity of $f_{t,\mu}$ yields

$$f_{t,\mu}(\mathbf{x}_t) - f_{t,\mu}(\mathbf{x}^*) \leq \langle \mathbb{E}_{\mathbf{u}}[\hat{\mathbf{g}}_t], \mathbf{x}_t - \mathbf{x}^* \rangle, \quad (77)$$

where we have used the fact that $\mathbb{E}_{\mathbf{u}}[\hat{\mathbf{g}}_t] = \nabla f_{t,\mu}(\mathbf{x}_t)$ given by Lemma A1. Taking the expectation with respect to all the randomness in (77), we then obtain

$$\mathbb{E}[f_{t,\mu}(\mathbf{x}_t) - f_{t,\mu}(\mathbf{x}^*)] \leq \mathbb{E}\langle \hat{\mathbf{g}}_t, \mathbf{x}_t - \mathbf{x}^* \rangle. \quad (78)$$

Further, recall that $\Pi_{\mathcal{X}, \sqrt{\hat{\mathbf{V}}_t}}(\mathbf{x}^*) = \arg \min_{\mathbf{x} \in \mathcal{X}} \|\hat{\mathbf{V}}_t^{1/4}(\mathbf{x} - \mathbf{x}^*)\|^2 = \mathbf{x}^*$, where for ease of notation, let $\|\cdot\|$ denote the Euclidean norm. Applying [18, Lemma 4] to ZO-AdaMM, we obtain that

$$\begin{aligned} \left\| \hat{\mathbf{V}}_t^{1/4}(\mathbf{x}_{t+1} - \mathbf{x}^*) \right\|^2 &\leq \left\| \hat{\mathbf{V}}_t^{1/4}(\mathbf{x}_t - \alpha_t \hat{\mathbf{V}}_t^{-1/2} \mathbf{m}_t - \mathbf{x}^*) \right\|^2 \\ &= \left\| \hat{\mathbf{V}}_t^{1/4}(\mathbf{x}_t - \mathbf{x}^*) \right\|^2 + \alpha_t^2 \|\hat{\mathbf{V}}_t^{-1/4} \mathbf{m}_t\|^2 - 2\alpha_t \langle \beta_{1,t} \mathbf{m}_{t-1} + (1 - \beta_{1,t}) \hat{\mathbf{g}}_t, \mathbf{x}_t - \mathbf{x}^* \rangle. \end{aligned} \quad (79)$$

Rearranging the above inequality, and using the Cauchy-Schwarz inequality $2\langle \mathbf{a}, \mathbf{b} \rangle \leq c\|\mathbf{a}\|^2 + \frac{1}{c}\|\mathbf{b}\|^2$ for $c > 0$, we obtain

$$\begin{aligned} \langle \hat{\mathbf{g}}_t, \mathbf{x}_t - \mathbf{x}^* \rangle &\leq \frac{\|\hat{\mathbf{V}}_t^{1/4}(\mathbf{x}_t - \mathbf{x}^*)\|^2 - \|\hat{\mathbf{V}}_t^{1/4}(\mathbf{x}_{t+1} - \mathbf{x}^*)\|^2}{2\alpha_t(1 - \beta_{1,t})} + \frac{\alpha_t \|\hat{\mathbf{V}}_t^{-1/4} \mathbf{m}_t\|^2}{2(1 - \beta_{1,t})} \\ &\quad + \frac{\beta_{1,t}}{1 - \beta_{1,t}} \frac{\alpha_t \|\hat{\mathbf{V}}_t^{-1/4} \mathbf{m}_{t-1}\|^2}{2} + \frac{\beta_{1,t}}{1 - \beta_{1,t}} \frac{\|\hat{\mathbf{V}}_t^{1/4}(\mathbf{x}_t - \mathbf{x}^*)\|^2}{2\alpha_t}. \end{aligned} \quad (80)$$

Taking the sum over t for (80), we obtain

$$\begin{aligned} \mathbb{E} \left[\sum_{t=1}^T \langle \hat{\mathbf{g}}_t, \mathbf{x}_t - \mathbf{x}^* \rangle \right] &\leq \frac{1}{2(1 - \beta_1)} \underbrace{\mathbb{E} \left[\sum_{t=1}^T \alpha_t \|\hat{\mathbf{V}}_t^{-1/4} \mathbf{m}_t\|^2 \right]}_A + \frac{\beta_1}{2(1 - \beta_1)} \underbrace{\mathbb{E} \left[\sum_{t=1}^T \alpha_t \|\hat{\mathbf{V}}_t^{-1/4} \mathbf{m}_{t-1}\|^2 \right]}_B \\ &\quad + \sum_{t=1}^T \mathbb{E} \left[\frac{\|\hat{\mathbf{V}}_t^{1/4}(\mathbf{x}_t - \mathbf{x}^*)\|^2 - \|\hat{\mathbf{V}}_t^{1/4}(\mathbf{x}_{t+1} - \mathbf{x}^*)\|^2}{2\alpha_t(1 - \beta_{1,t})} \right] + \sum_{t=1}^T \mathbb{E} \left[\frac{\beta_{1,t}}{2\alpha_t(1 - \beta_1)} \|\hat{\mathbf{V}}_t^{1/4}(\mathbf{x}_t - \mathbf{x}^*)\|^2 \right], \end{aligned} \quad (81)$$

where we have used the facts that $\beta_{1,t} \leq \beta_1$ and $1/(1 - \beta_{1,t}) \leq 1/(1 - \beta_1)$.

We next bound term A in (81). Based on (4), we can directly apply [18, Lemma 2] to obtain that

$$A \leq \frac{\alpha \sqrt{1 + \log T}}{(1 - \beta_1)(1 - \gamma) \sqrt{1 - \beta_2}} \sum_{i=1}^d \|\hat{\mathbf{g}}_{1:T,i}\|_2. \quad (82)$$

Furthermore, we bound term B in (81). Based on (4), we obtain that

$$\begin{aligned} B &= \sum_{t=1}^{T-1} \alpha_t \|\hat{\mathbf{V}}_t^{-1/4} \mathbf{m}_{t-1}\|^2 + \alpha_T \sum_{i=1}^d \frac{m_{T-1,i}^2}{\sqrt{\hat{v}_{T,i}}} \\ &\leq \sum_{t=1}^{T-1} \alpha_t \|\hat{\mathbf{V}}_t^{-1/4} \mathbf{m}_{t-1}\|^2 + \alpha_T \sum_{i=1}^d \frac{m_{T-1,i}^2}{\sqrt{v_{T,i}}}, \end{aligned} \quad (83)$$

where we have used the fact that $\mathbf{v}_t \leq \hat{\mathbf{v}}_t$ given in Algorithm 1. The last term in (83) can be further derived via (4),

$$\begin{aligned}
\alpha_T \sum_{i=1}^d \frac{m_{T-1,i}^2}{\sqrt{v_{T,i}}} &= \alpha \sum_{i=1}^d \frac{\left(\sum_{j=1}^{T-1} \left[\left(\prod_{k=1}^{T-j-1} \beta_{1,T-k} \right) \hat{g}_{j,i} (1 - \beta_{1,j}) \right] \right)^2}{\sqrt{T(1-\beta_2) \sum_{j=1}^T (\beta_2^{T-j} \hat{g}_{j,i}^2)}} \\
&\leq \alpha \sum_{i=1}^d \frac{\left(\sum_{j=1}^{T-1} \beta_1^{T-1-j} (1 - \beta_{1,j}) \right)^2 \left(\sum_{j=1}^{T-1} \beta_1^{T-1-j} \hat{g}_{j,i}^2 \right)}{\sqrt{T(1-\beta_2) \sum_{j=1}^T (\beta_2^{T-j} \hat{g}_{j,i}^2)}} \\
&\leq \alpha \sum_{i=1}^d \frac{\left(\sum_{j=1}^T \beta_1^{T-1-j} \right) \left(\sum_{j=1}^{T-1} \beta_1^{T-1-j} \hat{g}_{j,i}^2 \right)}{\sqrt{T(1-\beta_2) \sum_{j=1}^T (\beta_2^{T-j} \hat{g}_{j,i}^2)}} \\
&\leq \frac{\alpha}{(1-\beta_1)\sqrt{T(1-\beta_2)}} \sum_{i=1}^d \sum_{j=1}^T \frac{\beta_1^{T-1-j} \hat{g}_{j,i}^2}{\sqrt{\beta_2^{T-j} \hat{g}_{j,i}^2}} \\
&= \frac{\alpha}{\beta_1(1-\beta_1)\sqrt{T(1-\beta_2)}} \sum_{i=1}^d \sum_{j=1}^T \gamma^{T-j} |\hat{g}_{j,i}|, \tag{84}
\end{aligned}$$

where the first inequality holds due to Cauchy-Schwarz inequality and $\beta_{1,T-k} \leq \beta_1$ for $\forall k$, the second inequality holds due to $1 - \beta_{1,j} \leq 1$, and the third inequality holds due to $\sum_{j=1}^T \beta_1^{T-1-j} \leq 1/(1-\beta_1)$ and $\beta_2^{T-j} \hat{g}_{j,i}^2 \leq \sum_{j=1}^T \beta_2^{T-j} \hat{g}_{j,i}^2$. Based on (84), we then applies the proof of [18, Lemma 2], which yields

$$B \leq \frac{\alpha \sqrt{1 + \log T}}{\beta_1(1-\beta_1)(1-\gamma)\sqrt{1-\beta_2}} \sum_{i=1}^d \|\hat{\mathbf{g}}_{1:T,i}\|_2 \tag{85}$$

Substituting (82) and (85) into (81), we obtain that

$$\begin{aligned}
\mathbb{E} \left[\sum_{t=1}^T \langle \hat{\mathbf{g}}_t, \mathbf{x}_t - \mathbf{x}^* \rangle \right] &\leq \frac{\alpha \sqrt{1 + \log T} \sum_{i=1}^d \mathbb{E} \|\hat{\mathbf{g}}_{1:T,i}\|}{(1-\beta_1)^2(1-\gamma)\sqrt{1-\beta_2}} \\
+ \mathbb{E} \left[\underbrace{\sum_{t=1}^T \frac{\|\hat{\mathbf{V}}_t^{1/4}(\mathbf{x}_t - \mathbf{x}^*)\|^2 - \|\hat{\mathbf{V}}_t^{1/4}(\mathbf{x}_{t+1} - \mathbf{x}^*)\|^2}{2\alpha_t(1-\beta_{1,t})}}_C \right] &+ \mathbb{E} \left[\underbrace{\sum_{t=1}^T \frac{\beta_{1,t} \|\hat{\mathbf{V}}_t^{1/4}(\mathbf{x}_t - \mathbf{x}^*)\|^2}{2\alpha_t(1-\beta_1)}}_D \right]. \tag{86}
\end{aligned}$$

In (86), the term D yields

$$D \leq \frac{\beta_1 D_\infty^2}{2(1-\beta_1)} \sum_{t=1}^T \sum_{i=1}^d \frac{\hat{v}_{t,i}^{1/2}}{\alpha_t}. \tag{87}$$

We remark that it was shown in [39] that the proof in [18] to bound the term C is problematic. Compared to [39], we propose a simpler fix to bound C when $0 < \beta_{1,t} \leq \beta_{1,t-1} \leq 1$. We rewrite C in (86) as

$$\begin{aligned}
C &= \frac{\|\hat{\mathbf{V}}_1^{1/4}(\mathbf{x}_1 - \mathbf{x}^*)\|^2}{2\alpha_1(1-\beta_{1,1})} + \sum_{t=2}^T \frac{\|\hat{\mathbf{V}}_t^{1/4}(\mathbf{x}_t - \mathbf{x}^*)\|^2}{2\alpha_t(1-\beta_{1,t})} \\
&\quad - \sum_{t=2}^T \frac{\|\hat{\mathbf{V}}_{t-1}^{1/4}(\mathbf{x}_t - \mathbf{x}^*)\|^2}{2\alpha_{t-1}(1-\beta_{1,t-1})} - \frac{\|\hat{\mathbf{V}}_T^{1/4}(\mathbf{x}_{T+1} - \mathbf{x}^*)\|^2}{2\alpha_T(1-\beta_{1,T})} \\
&= \sum_{t=2}^T \left[\frac{\|\hat{\mathbf{V}}_t^{1/4}(\mathbf{x}_t - \mathbf{x}^*)\|^2}{2\alpha_t(1-\beta_{1,t})} - \frac{\|\hat{\mathbf{V}}_{t-1}^{1/4}(\mathbf{x}_t - \mathbf{x}^*)\|^2}{2\alpha_{t-1}(1-\beta_{1,t-1})} \right] \\
&\quad + \frac{\|\hat{\mathbf{V}}_1^{1/4}(\mathbf{x}_1 - \mathbf{x}^*)\|^2}{2\alpha_1(1-\beta_{1,1})} - \frac{\|\hat{\mathbf{V}}_T^{1/4}(\mathbf{x}_{T+1} - \mathbf{x}^*)\|^2}{2\alpha_T(1-\beta_{1,T})}. \tag{88}
\end{aligned}$$

Further, the first term in RHS of (88) can be bounded as

$$\begin{aligned}
& \sum_{t=2}^T \left[\frac{\|\hat{\mathbf{V}}_t^{1/4}(\mathbf{x}_t - \mathbf{x}^*)\|^2}{2\alpha_t(1 - \beta_{1,t})} - \frac{\|\hat{\mathbf{V}}_{t-1}^{1/4}(\mathbf{x}_t - \mathbf{x}^*)\|^2}{2\alpha_{t-1}(1 - \beta_{1,t-1})} \right] \\
&= \sum_{t=2}^T \left[\frac{\|\hat{\mathbf{V}}_t^{1/4}(\mathbf{x}_t - \mathbf{x}^*)\|^2}{2\alpha_t(1 - \beta_{1,t})} - \frac{\|\hat{\mathbf{V}}_{t-1}^{1/4}(\mathbf{x}_t - \mathbf{x}^*)\|^2}{2\alpha_{t-1}(1 - \beta_{1,t})} \right] \\
&\quad + \sum_{t=2}^T \left[\left(\frac{1}{1 - \beta_{1,t}} - \frac{1}{1 - \beta_{1,t-1}} \right) \frac{\|\hat{\mathbf{V}}_{t-1}^{1/4}(\mathbf{x}_t - \mathbf{x}^*)\|^2}{2\alpha_{t-1}} \right] \\
&\stackrel{(a)}{\leq} \frac{1}{2(1 - \beta_1)} \sum_{t=2}^T \left[\sum_{i=1}^d \left(\frac{\hat{v}_{t,i}^{1/2}(x_{t,i} - x_i^*)^2}{\alpha_t} - \frac{\hat{v}_{t-1,i}^{1/2}(x_{t,i} - x_i^*)^2}{\alpha_{t-1}} \right) \right] \\
&\stackrel{(b)}{\leq} \frac{D_\infty^2 \sum_{i=1}^d \sum_{t=2}^T \left[\frac{\hat{v}_{t,i}^{1/2}}{\alpha_t} - \frac{\hat{v}_{t-1,i}^{1/2}}{\alpha_{t-1}} \right]}{2(1 - \beta_1)} \leq \frac{D_\infty^2 \sum_{i=1}^d \hat{v}_{T,i}^{1/2}}{2\alpha_T(1 - \beta_1)} \tag{89}
\end{aligned}$$

where the inequality (a) holds since $\beta_{1,t} \leq \beta_{1,t-1} \leq \beta_1$ and $1/(1 - \beta_{1,t}) - 1/(1 - \beta_{1,t-1}) \leq 0$, and the inequality (b) holds due to $\|x_t - x^*\|_\infty \leq D_\infty$ and $\frac{\hat{v}_{t,i}^{1/2}}{\alpha_t} - \frac{\hat{v}_{t-1,i}^{1/2}}{\alpha_{t-1}} \geq 0$. Substituting (89) into (88), we obtain that

$$C \leq \frac{D_\infty^2 \sum_{i=1}^d \hat{v}_{T,i}^{1/2}}{2\alpha_T(1 - \beta_1)} + \frac{D_\infty^2 \sum_{i=1}^d \hat{v}_{1,i}^{1/2}}{2\alpha_1(1 - \beta_1)} \leq \frac{D_\infty^2 \sum_{i=1}^d \hat{v}_{T,i}^{1/2}}{\alpha_T(1 - \beta_1)}, \tag{90}$$

where the last inequality holds since $\hat{v}_{t+1,i}^{1/2} \geq \hat{v}_{t,i}^{1/2}$ and $\alpha_1 \geq \alpha_T$.

We highlight that although the proof on bounding C in [18, Theorem 4] is problematic, the conclusion of [18, Theorem 4] keeps correct.

Substituting C and D into (86), we obtain that

$$\begin{aligned}
\mathbb{E} \left[\sum_{t=1}^T \langle \hat{\mathbf{g}}_t, \mathbf{x}_t - \mathbf{x}^* \rangle \right] &\leq \frac{\alpha \sqrt{1 + \log T} \sum_{i=1}^d \mathbb{E} \|\hat{\mathbf{g}}_{1:T,i}\|}{(1 - \beta_1)^2 (1 - \gamma) \sqrt{1 - \beta_2}} \\
&+ \frac{D_\infty^2 \sum_{i=1}^d \mathbb{E}[\hat{v}_{T,i}^{1/2}]}{\alpha_T(1 - \beta_1)} + \frac{D_\infty^2}{2(1 - \beta_1)} \sum_{t=1}^T \sum_{i=1}^d \frac{\beta_{1,t} \mathbb{E}[\hat{v}_{t,i}^{1/2}]}{\alpha_t}. \tag{91}
\end{aligned}$$

In (91), since $\sqrt{\cdot}$ is a concave function, the Jensen's inequality yields

$$\mathbb{E}[\sqrt{\hat{v}_{t,i}}] \leq \sqrt{\mathbb{E}[\hat{v}_{t,i}]}. \tag{92}$$

Substituting (92) into (91) and (78), we complete the proof. \square

4 Supplementary Material of Experiments

4.1 Problem and experiment setup

It is known that DNN-based image classifiers are vulnerable to adversarial examples—one can carefully craft images with imperceptible perturbations (a.k.a. adversarial perturbations or adversarial attacks) that can fool image classifiers even under a *black box* threat model, where details of the model are unknown to the attacker [5, 6, 48, 49].

We focus on two problem settings of black-box adversarial attacks: per-image adversarial perturbation and universal adversarial perturbation. Let (\mathbf{x}, t) denote a legitimate image \mathbf{x} with the true label $t \in \{1, 2, \dots, K\}$, where K is the total number of image classes. And let $\mathbf{x}' = \mathbf{x} + \delta$ denote an adversarial example, where δ is the adversarial perturbation. Our goal is to design δ for a single

image \mathbf{x} or multiple images $\{\mathbf{x}_i\}_{i=1}^M$. Spurred by [51], we consider the optimization problem

$$\begin{aligned} & \underset{\boldsymbol{\delta}}{\text{minimize}} && \frac{\lambda}{M} \sum_{i=1}^M f(\mathbf{x}_i + \boldsymbol{\delta}) + \|\boldsymbol{\delta}\|_2^2 \\ & \text{subject to} && (\mathbf{x}_i + \boldsymbol{\delta}) \in [-0.5, 0.5]^d, \forall i, \end{aligned} \quad (93)$$

where $f(\mathbf{x}_0 + \boldsymbol{\delta})$ denotes the (black-box) attack loss function, $\lambda > 0$ is a regularization parameter that strikes a balance between minimizing the attack loss and the ℓ_2 distortion, and we normalize the pixel values to $[-0.5, 0.5]^d$. In problem (93), we specify the loss function for untargeted attack [51], $f(\mathbf{x}') = \max\{Z(\mathbf{x}')_t - \max_{j \neq t} Z(\mathbf{x}')_j, -\kappa\}$, where $Z(\mathbf{x}')_k$ denotes the prediction score of class k given the input \mathbf{x}' , and the parameter $\kappa > 0$ governs the gap between the confidence of the predicted label and the true label t . In experiments, we choose $\kappa = 0$, and the attack loss f reaches the minimum value 0 as the perturbation succeeds to fool the neural network.

In problem (93), if $M = 1$, then it becomes our first task to find per-image adversarial perturbations. If $M > 1$, then the problem corresponds to the task of finding universal adversarial perturbations to M images. Problem (93) yields a constrained formulation for the design of black-box adversarial attacks. Since some ZO algorithms are designed only for unconstrained optimization (see Table 1), we also consider the unconstrained version of problem (93) [24],

$$\begin{aligned} & \underset{\mathbf{w} \in \mathbb{R}^d}{\text{minimize}} && \frac{\lambda}{M} \sum_{i=1}^M [f(0.5 \tanh(\tanh^{-1}(2\mathbf{x}_i) + \mathbf{w})) \\ & && + \|\mathbf{w}\|_2^2], \end{aligned} \quad (94)$$

where $\mathbf{w} \in \mathbb{R}^d$ are optimization variables, and we eliminate the inequality constraint in (93) by leveraging $0.5 \tanh(\tanh^{-1}(2\mathbf{x}_i) + \mathbf{w}) = \mathbf{x}_i + \boldsymbol{\delta} \in [-0.5, 0.5]^d$.

The experiments of generating black-box adversarial examples will be performed on Inception V3 [45] under the dataset ImageNet [46]. We will compare the proposed ZO-AdaMM method with 6 existing ZO algorithms, ZO-SGD [9], ZO-SCD [22] and ZO-signSGD [14] for unconstrained optimization, and ZO-PSGD [27], ZO-SMD [23] and ZO-NES [6] for constrained optimization. The first 5 methods have been summarized in Table 1, and ZO-NES refers to the black-box attack generation method in [6], which applies a projected version of ZO-signSGD using natural evolution strategy (NES) based random gradient estimator. In all the aforementioned ZO algorithms, we adopt the random gradient estimator (14) and set $b = 1$ and $q = 10$ so that every method takes the same query cost per iteration. Accordingly, the total query complexity is consistent with the number of iterations.

In Fig. A1, we show the influence of exponential averaging parameters β_1 and β_2 on the convergence of ZO-AdaMM, in terms of the converged total loss while designing the per-image (ID 11 in ImageNet) and universal adversarial attack. As we can see, the typical choice of $\beta_2 > 0.9$ is no longer the empirically optimal choice in the ZO setting. In all of our experiments, we find that the choice of $\beta_1 \geq 0.9$ and $\beta_2 \in [0.3, 0.5]$ performs well in practice. In Table A1 and A2, we present the best learning rate parameter α founded by greedy search at each experiment, in the sense that the smallest objective function (corresponding to the successful attack) is achieved given the maximum number of iterations T .

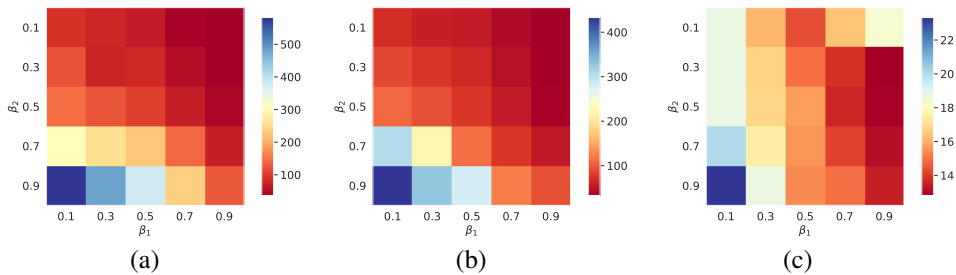


Figure A1: The heat map of the converged objective value at 1000 iterations versus different combinations of β_1 and β_2 of ZO-AdaMM. (a) Unconstrained per-image (ID 11) adversarial attack problem (94); (b) Constrained per-image (ID 11) adversarial attack problem (93); (c) Universal adversarial attack problem (93) with $M = 10$.

| Methods | Learning rate α | Converged objective value | Success of attack |
|------------|------------------------|---------------------------|-------------------|
| ZO-PSGD | 4×10^{-4} | 245.92 | × |
| | 2×10^{-4} | 78.66 | ✓ |
| | 1×10^{-4} | 31.42 | ✓ |
| | 9×10^{-5} | 30.98 | × |
| ZO-SMD | 8×10^{-4} | 245.92 | × |
| | 5×10^{-4} | 97.42 | ✓ |
| | 3×10^{-4} | 35.19 | ✓ |
| | 9×10^{-5} | 36 | × |
| ZO-NES | 5×10^{-2} | 3997 | × |
| | 1×10^{-2} | 194.22 | ✓ |
| | 9×10^{-3} | 158.02 | ✓ |
| | 8×10^{-3} | 129.30 | × |
| ZO-SCD | 8×10^{-3} | 330.12 | × |
| | 2×10^{-3} | 77.14 | ✓ |
| | 1×10^{-3} | 42.87 | ✓ |
| | 9×10^{-3} | 39.60 | × |
| ZO-SGD | 5×10^{-3} | 1089.57 | × |
| | 8×10^{-4} | 33.60 | ✓ |
| | 5×10^{-4} | 31.11 | ✓ |
| | 4×10^{-4} | 33.13 | × |
| ZO-signSGD | 8×10^{-2} | 1590.02 | × |
| | 2×10^{-2} | 113.43 | ✓ |
| | 1×10^{-2} | 41.96 | ✓ |
| | 9×10^{-3} | 39.60 | × |

Table A1: Greedy search on the best learning rate parameter α for generating per-image adversarial perturbations.

| Methods | Learning rate α | Converged objective value | Success of attack |
|---------|------------------------|---------------------------|-------------------|
| ZO-PSGD | 1×10^{-2} | 1072.05 | × |
| | 1×10^{-3} | 147.46 | ✓ |
| | 4×10^{-4} | 56.99 | ✓ |
| | 3×10^{-4} | 36.86 | ✓ |
| | 2×10^{-5} | 24.91 | × |
| ZO-SMD | 1×10^{-2} | 788.46 | × |
| | 1×10^{-3} | 60.98 | ✓ |
| | 6×10^{-4} | 36.86 | ✓ |
| | 5×10^{-4} | 29.56 | ✓ |
| | 4×10^{-4} | 24.91 | × |
| ZO-NES | 1×10^{-2} | 1230.15 | × |
| | 4×10^{-2} | 107.74 | ✓ |
| | 7×10^{-3} | 65.64 | ✓ |
| | 6×10^{-3} | 54.00 | ✓ |
| | 5×10^{-3} | 42.57 | × |

Table A2: Greedy search on the best learning rate parameter α for design of universal adversarial perturbations by solving problem (93).

4.2 Per-image black-box adversarial attack

We consider the task of per-image adversarial perturbation by solving problems (93) and (94), where $M = 1$ and $\lambda = 10$. In ZO-AdaMM (Algorithm 1), we set $\mathbf{v}_0 = \hat{\mathbf{v}}_0 = 10^{-5}$, $\mathbf{m}_0 = \mathbf{0}$, $\beta_{1t} = \beta_1 = 0.9$, $\beta_2 = 0.3$ and $T = 1000$. Here the exponential moving average parameters (β_1, β_2) are exhaustively searched over $\{0.1, 0.3, 0.5, 0.7, 0.9\}^2$; see Fig. A1-(a) & (b) in Appendix 4 as an example. In ZO-AdaMM, we also choose a decaying learning rate $\alpha_t = \alpha/\sqrt{t}$ with $\alpha = 0.01$. For fair comparison, we use the decaying strategy for all other ZO algorithms, and we determine the best choice of α by greedy search over the interval $[10^{-4}, 10^{-2}]$; see Table A1 in Appendix 4 for more results on selecting α .

In Table A3, we summarize the key statistics of each ZO optimization method for solving the per-image adversarial attack problem over 100 images randomly selected from ImageNet. For solving the unconstrained problem (94), ZO-SCD has the worst attack performance in general, i.e., leading to the largest number of iterations to reach the first successful attack and the largest final distortion.

We also observe that ZO-signSGD and ZO-AdaMM achieve better attack performance. However, the downside of ZO-signSGD is its poor convergence accuracy, given by the increase in distortion from the first successful attack to the final attack (i.e., 23.00 \rightarrow 28.52 in Table A3). For solving the constrained problem (93), ZO-AdaMM achieves the best attack performance except for a slight drop in the attack success rate (ASR). Similar to ZO-signSGD, ZO-NES has a poor convergence accuracy in terms of the increase in ℓ_2 distortion after the attack becomes successful.

| Problem | Methods | ASR | Ave. iters (1st succ.) | $\ \delta_t\ _2^2$ (1st succ.) | Final $\ \delta_T\ _2^2$ |
|---------|------------|------------|---------------------------|-----------------------------------|-----------------------------|
| (94) | ZO-SCD | 78% | 240 | 57.88 | 57.51 |
| | ZO-SGD | 78% | 159 | 38.36 | 37.85 |
| | ZO-signSGD | 74% | 179 | 23.00 | 28.52 |
| | ZO-AdaMM | 81% | 173 | 28.58 | 28.20 |
| (93) | ZO-NES | 82% | 229 | 82.78 | 84.41 |
| | ZO-PSGD | 78% | 112 | 60.32 | 58.10 |
| | ZO-SMD | 76% | 198 | 35.08 | 35.05 |
| | ZO-AdaMM | 78% | 197 | 23.77 | 23.72 |

Table A3: Performance of per-image attack over 100 images under $T = 1000$ iterations, where ASR represents attack success rate, and the distortion $\|\delta\|_2^2$ is averaged over successful attacks only.

4.3 Universal black-box adversarial attack

In this experiment, we solve the constrained problem (93) for designing a universal adversarial perturbation δ , where we attack $M = 10$ images with the true class label ‘brambling’ and we set $\lambda = 10$ in (93). The setting of algorithmic parameters is similar to Appendix 4.2 except $T = 20000$. For ZO-AdaMM, we choose $\alpha = 0.002$, $\beta_1 = 0.9$, and $\beta_2 = 0.3$, where the sensitivity of exponential moving average parameters (β_1, β_2) is shown in Fig. A1-(c). For the other ZO algorithms, we greedily search α over $[10^{-2}, 10^{-4}]$ and choose the value that achieves the best convergence accuracy as shown in Table A2.

In Fig. A2, we visualize the pattern of universal adversarial perturbation obtained from different methods. As we can see, the resulting universal perturbation pattern identifies the most discriminative image regions corresponding to the true label ‘brambling’. We also observe that although each method successfully generates the black-box adversarial example, ZO-AdaMM yields the strongest attack that requires the least distortion strength.

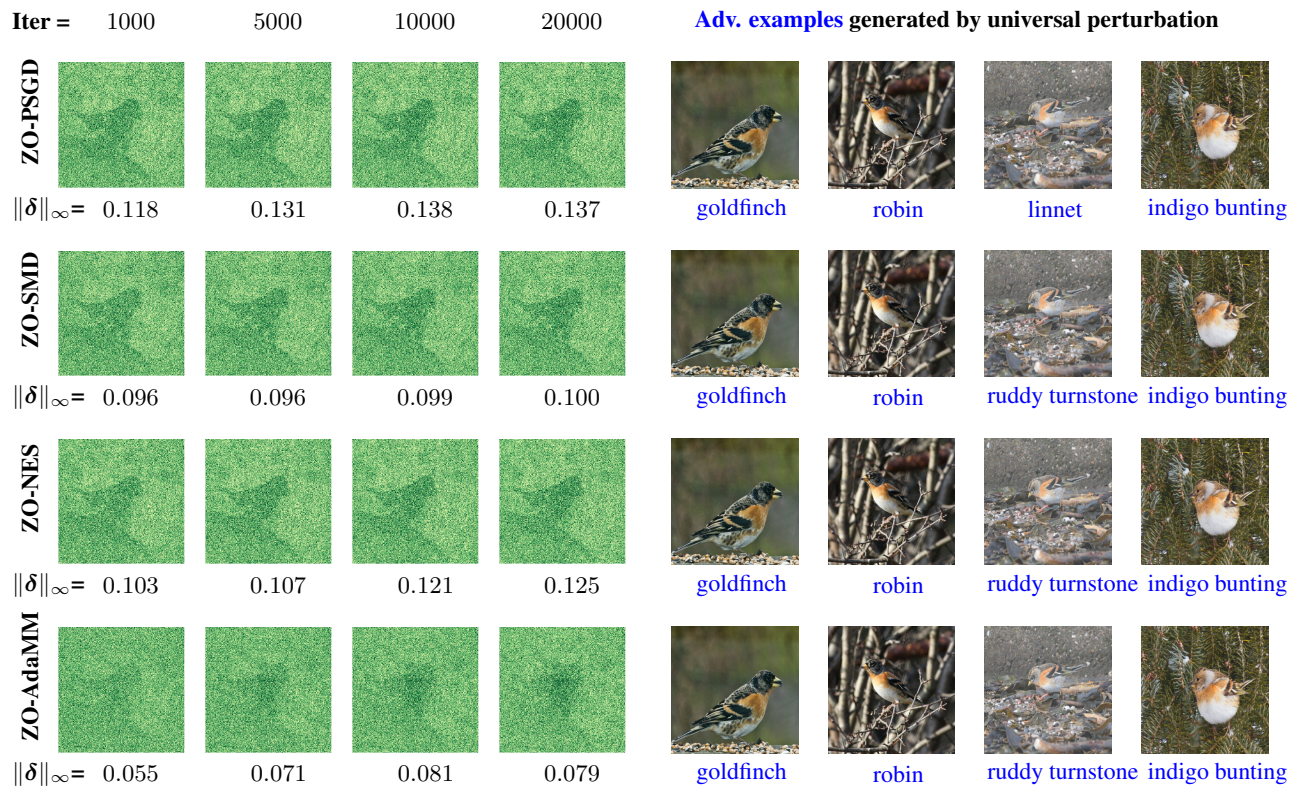


Figure A2: Visualization of universal perturbation versus different iterations and the eventually generated adversarial examples. Left four columns present universal perturbations found by different ZO algorithms at the iteration number 1000, 5000, 10000 and 20000, where the depth of the color corresponds to the strength of the perturbation, and the maximum distortion $\|\delta\|_\infty$ (with deepest green) is given at the bottom of each subplot. The right four columns are 4 of 10 adversarial examples that lead to missclassification from the original label ‘brambling’ to an incorrectly predicted label given at the bottom of each subplot.